



Effect of Au and/or Mo Doping on the Development of Carbon and Sulfur Tolerant Anodes for SOFCs—A Short Review

Dimitrios K. Niakolas¹, Charalambos S. Neofytidis^{1,2} and Stylianos G. Neophytides^{1*}

¹ Foundation for Research and Technology, Institute of Chemical Engineering Sciences, Patras, Greece, ² Department of Chemical Engineering, University of Patras, Patras, Greece

HIGHLIGHTS

- The kinetics of CH₄ steam reforming and partial oxidation are determined by the oxidation rate of CH_x adsorbed species
- The modification of the Ni/YSZ and Ni/GDC with Au and/or Au-Mo results in differentiated structures of atomically dispersed Au and/or Au-Mo at the surface and the bulk of the Ni particles.
- At lean S/C NiAu/YSZ selectively oxidizes electrochemically the catalytically produced H₂ and CO, while NiAu/GDC is selective to the direct partial electrochemical oxidation of CH₄ to CO and H₂.
- The modified electrodes show significant tolerance to C formation.
- Au-Mo modification enhances the intrinsic sulfur tolerance properties of Ni/GDC.

The presented work is a short review of the research attempts from our group with collaborators, during the last 15 years, which had as main objective to study and improve the electrocatalytic performance of Ni-based electrode materials for the CH₄ Internal steam Reforming process (ISR.) in Solid Oxide Fuel Cells (SOFCs). In particular, NiO/YSZ and NiO/GDC anode powders were modified with Au and/or Mo nano-particles via different preparation methods. These efforts resulted in anode materials with high tolerance and improved electrocatalytic activity under both carbon forming and sulfur poisoning conditions. The most important findings are being reviewed and critical findings are being highlighted 50 as to stress the key differences in the electrocatalytic performance between Ni/YSZ and Ni/GDC. The possible effects of Au and/or Mo addition on the physicochemical and structural properties of the cermets are thoroughly discussed as well as active functional layers in the form of anode SOFC electrodes.

Keywords: SOFCs, Ni/YSZ, Ni/GDC, Au-Mo-modification, carbon tolerance, sulfur poisoning, CH₄ internal steam reforming

OPEN ACCESS

Edited by:

Kostas A. Komnitsas,
Technical University of Crete, Greece

Reviewed by:

Michalis I. Konsolakis,
Technical University of Crete, Greece
Stephen Skinner,
Imperial College London,
United Kingdom

*Correspondence:

Stylianos G. Neophytides
neoph@iceht.forth.gr

Specialty section:

This article was submitted to
Wastewater Management,
a section of the journal
Frontiers in Environmental Science

Received: 12 July 2017

Accepted: 01 November 2017

Published: 14 November 2017

Citation:

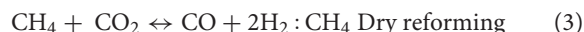
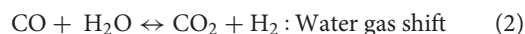
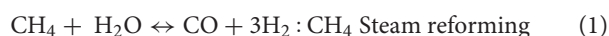
Niakolas DK, Neofytidis CS and
Neophytides SG (2017) Effect of Au
and/or Mo Doping on the
Development of Carbon and Sulfur
Tolerant Anodes for SOFCs—A Short
Review. *Front. Environ. Sci.* 5:78.
doi: 10.3389/fenvs.2017.00078

INTRODUCTION

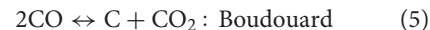
Solid Oxide fuel Cells (SOFCs) are considered as one of the most attractive and efficient fuel cell technology for the generation of clean power, by converting chemical energy directly into electricity. The main advantages that renders them so efficient are: (i) their high electrical efficiency due to the enhanced reaction kinetics within the high and wide operating temperature range (500–1,000°C), (ii) fuel flexibility (direct use of hydrocarbon feedstocks), and (iii) production of high quality waste heat so as to be used for efficient Combined Heat and Power (CHP) applications (Singh and Hill, 2012; Niakolas, 2014). SOFCs can be fed directly with various hydrocarbon (H/C) fuels, omitting the use of external reformer. This mode of operation, known as Internal Reforming (I.R.), is the main competitive advantage for the commercialization of SOFCs mainly as CHP units for stationary applications. Their operation as such improves and simplifies the whole system's integration. Specifically, I.R. is based on the catalytic activity of the anode electrode at the high operating temperatures and the main benefit is that part of the generated heat in the cell, can be readily used for the endothermic reforming reactions (Mogensen et al., 2011; Singh and Hill, 2012; Niakolas, 2014). Thus, various types of H/C fuels can be used, including biogas and Natural Gas (N.G.). However, the basic drawback is focused on the carbon deposition processes and containing sulfur impurities, which deactivate the State of the Art (SoA) SOFC anodes (Hagen, 2013; Niakolas, 2014).

Ni-containing cermets with Ytria Stabilized Zirconia (YSZ), Scandia Stabilized Zirconia (ScSZ), and Gadolinia Doped Ceria (GDC) are currently the most commonly used anode materials. At the operating conditions of SOFCs, Ni-based electrodes exhibit very good catalytic activity for the reforming reactions and high electronic conductivity for the facilitation of the electrochemical oxidation of H₂ as well as high gas diffusivity and excellent mechanical/structural integrity. The commercial interest on the I.R. mode of operation urged the SOFC community to focus on these materials, owing to their close relation with the typical nickel-containing reforming catalysts (Niakolas, 2014). However, SOFCs comprising Ni-based anodes are characterized by some critical degradations issues. Indicatively: (i) they are prone to carbon deposition, which is created by the decomposition of e.g., CH₄ [reaction (4)] and/or of CO disproportionation Boudouart [reaction (5)], (ii) the corrosion caused on Ni by the deposited carbon, thus leading to structural damage of the conductive percolation pathways of the anode and the loss of its conductivity (Chen et al., 2011; Singh and Hill, 2012), (iii) they exhibit poor redox stability, and (iv) on the long term Ni forms agglomerates with detrimental consequences on the electronic conductivity (Faes et al., 2009).

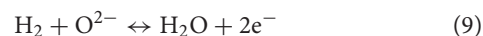
The internal steam reforming of methane for the production of H₂, CO, and CO₂, is an endothermic process. It can be assumed as a mixture of the following catalytic and electrochemical reactions, which proceed in parallel and/or in series (Maier et al., 2011; Niakolas et al., 2013; Souentie et al., 2013):



At temperatures, typically below 700°C, CO can undergo disproportionation [reaction (5)] and forms carbon.



As far as the electrochemical reactions are concerned, H₂ and CO can be oxidized at the solid state electrochemical interface [electrolyte/metal/gas three-phase boundaries (tpb)] to form H₂O and CO₂ (reactions 9 and 10).



In addition, CH₄ can be partially oxidized electrochemically toward the production of H₂ and CO (Bebelis et al., 2000, 2006; Souentie et al., 2013).



Taking into consideration the above, carbon formation can take place through reactions (4) and (5) and the reverse of (6). On the other hand, carbon removal is facilitated through reactions (6) and (7) and the reverse of (5). Overall, carbon accumulation takes place in the case where the rate of carbon forming reactions exceeds the rate of carbon removal reactions (Singh and Hill, 2012).

Thus, the SOFC I.R. operation mode can be feasible (Niakolas, 2014; Florea et al., in press) if the anode electrode is active for the reforming reactions and tolerant against carbon formation. This is rather difficult for Ni-based materials and especially for Ni/YSZ, which is the SoA anode for both electrolyte and electrode-supported cells. A typical approach that is being followed in order to avoid carbon deposits is to increase the steam content in the fuel and to maintain a steam/carbon (S/C) ratio equal to 2 or higher. However, such S/C ratios appear rather to be too high for practical reasons in SOFCs due to the significant decrease in the Nernst potential and the possibility to oxidize the anode with detrimental effect on its electronic conductivity (Mogensen et al., 2011).

Therefore, the development of efficient and carbon tolerant anodes, aiming to replace Ni/YSZ is a demanding prerequisite for the effective processing of hydrocarbon feedstocks and especially natural gas in SOFCs. A vast number of published studies can be summarized with a selection of other anode candidates such as: (a) Ru (Sauvet and Fouletier, 2001; Bebelis et al., 2006; Caillot et al., 2007), (b) Cu (Slater and Irvine, 1999; Park et al., 2000), (c) Fluorite (e.g., Cu–CeO₂–ScSZ; Ye et al., 2007), (d) Tungsten bronze (e.g., (Ba/Sr/Ca/La)_{0.6}M_xNb_{1-x}O_{3-δ}, where M=Mg, Ni, Mn, Cr, Fe, In, Ti, Sn; Tao and Irvine, 2004), (e)

Pyrochlore (e.g., $\text{Gd}_2\text{Ti}_2\text{O}_7$) anode materials (Goodenough and Huang, 2007; Sun and Stimming, 2007; Tsipis and Kharton, 2008), (f) LSCM (e.g., $\text{La}_{0.75}\text{Sr}_{0.25}\text{Cr}_{0.5}\text{Mn}_{0.5}\text{O}_{3-\delta}$) (Sfeir et al., 2001; Liu et al., 2002; Tao and Irvine, 2004; Ruiz-Morales et al., 2007), SrMoO_4 (Smith and Gross, 2011), and other complex perovskites (Xiao et al., 2010), such as double perovskites (e.g., $\text{Sr}_2\text{Mg}_{1-x}\text{Mn}_x\text{MoO}_{6-\delta}$; Huang et al., 2006 or $\text{Sr}_2\text{CoMoO}_6$; Zhang et al., 2011), chromites (Vashook et al., 2003), and titanates (Li X. et al., 2009). Although most of the above materials are characterized by high carbon resistance, nevertheless, in most of the cases their practical use is inhibited by the poor electrochemical or catalytic activity, the relatively low electronic conduction, the low thermal and chemical stability, the use of prohibitively expensive materials and/or the high cost of processing for their commercial use (Tsipis and Kharton, 2008; Niakolas et al., 2010). Among the cermet materials Cu/YSZ or Cu-CeO₂-YSZ were proven as a promising carbon tolerant material, however it appears to be rather problematic due to sintering at high operating temperatures (Kim et al., 2002; Gorte and Vohs, 2003; Atkinson et al., 2004; Krishnan et al., 2004; Costa-Nunes et al., 2005).

In particular CeO_{2- δ} -based formulations have been considered as quite promising materials. The reduced form of ceria exhibits a substantial mixed oxygen ionic and n-type electronic conductivity with high oxygen storage and exchange capacity and the extraordinary mechanical and thermal stability properties of ceria even during redox procedures. In addition CeO₂ based supports are considered very active with strong metal support interactions and synergistic kinetic promotional effects (Goodenough and Huang, 2007; Niakolas, 2014) especially for internal reforming operation in SOFCs. In this category GDC [$\text{CeO}_2(\text{Gd}_2\text{O}_3)$] is one of the most frequently used substitutes of YSZ. It inhibits coke formation and for it is catalytically active in the steam reforming of methane (Ramirez-Cabrera et al., 2004; Niakolas, 2014; Florea et al., in press). Nevertheless, GDC alone is inactive for the processing of CH₄ activation. The formation of cermet after mixing with nickel oxide to form Ni/GDC after NiO reduction is rendered a highly potential electrode for CH₄ fueled SOFCs.

The performance of Ni/YSZ and Ni/GDC as anodes in H/C fueled SOFCs can be improved by dispersing uniformly small amounts of either transition non-noble—metal additives (Sn, Kan et al., 2009; Kan and Lee, 2010a), Cu (Gorte et al., 2000; Hornés et al., 2007; Sin et al., 2007), Mo (Finnerty et al., 1998; An et al., 2011; Niakolas et al., 2013), Bi (Huang et al., 2009), and Fe (Park and Virkar, 2009; da Paz Fiuza et al., 2010; Kan and Lee, 2010b; Fu et al., 2011) or noble-metal dopands (Ru, Hibino et al., 2003; Modafferi et al., 2008), Pd (Nabae et al., 2006, 2008; Babaei et al., 2009), Rh (Hibino et al., 2002b; Boaro et al., 2010; Ferrandon et al., 2010), Pt (Hibino et al., 2002a), and Au (Yentekakis, 2006; Gavrielatos et al., 2008; Yentekakis et al., 2008), which appear to be effective at intermediate operating temperatures (Rostrup-Nielsen and Alstrup, 1999; Goodenough and Huang, 2007). The aim of these research efforts was to enhance carbon tolerance and maintain catalytic performance through the formation of bimetallic alloys with Ni on the anode.

Besenbacher et al. (1998) concluded that Ni-Au alloys containing small amount of atomically dispersed gold on the Ni surface can decrease significantly the amount of carbon deposits on Ni based CH₄ steam reforming catalysts. This was also predicted theoretically by means of density functional theory (DFT) calculations carried out by Rostrup-Nielsen et al. (Rostrup-Nielsen and Alstrup, 1999). They found that methane dissociation into carbon is significantly inhibited.

Regarding sulfur tolerance early efforts were initiated on H₂S/air fuel cell and MCFC systems (Pujare et al., 1987; Weaver and Winnick, 1989; Yentekakis and Vayenas, 1989; Gong et al., 2007; Vorontsov et al., 2008). MoS₂, NiS, and NiMoS₂-Ag/YSZ were mainly examined as anode materials. The vast literature refers and focusses on systems, which are fed with H₂S in H₂-containing fuels. They studied the deactivation mechanisms and materials application (Cheng et al., 2007; Zha et al., 2007; Li T. S. et al., 2009; Li et al., 2010; Rasmussen and Hagen, 2009, 2010; Xu et al., 2010; Li and Wang, 2011a,b), summarized in several studies and reviews (Sasaki et al., 2006, 2011; Tremblay et al., 2006; Gong et al., 2007; Goodenough and Huang, 2007; Sun and Stimming, 2007; Rasmussen and Hagen, 2009; Yang et al., 2010; Cheng et al., 2011; Hagen et al., 2011; Kromp et al., 2012; Hagen, 2013; Wang et al., 2013; Weber et al., 2013; Hauch et al., 2014). The effect of a sulfur-containing fuel is examined on the performance and durability of SOFCs through the variation of several factors, such as the: (i) operating temperature, (ii) applied current/voltage load, (iii) time on stream, (iv) H₂S concentration and to a lesser extent the concentration of H₂ and H₂O, and (v) the anodes materials. The most significant degradation effect is the drop in the cell voltage and thus, of the SOFC performance.

In the present manuscript a conclusive review will be presented on the activities of our group describing the roadmap toward the development of carbon tolerant and sulfur tolerant Ni based anode electrodes by doping Ni cermets with Au and Mo. In this direction our research group with collaborators (Niakolas et al., 2010, 2013, 2015; Papaefthimiou et al., 2013; Souentie et al., 2013; Neofytidis et al., 2015) attempted to study and modify NiO/YSZ and NiO/GDC powder with Au and/or Mo nano-particles. These modifications resulted in electrodes with high tolerance and improved electrocatalytic activity under both carbon forming and sulfur poisoning conditions. One of the main findings was the induced structural modification on nickel through the formation of bimetallic Au-Ni and ternary Au-Mo-Ni solid solutions. Furthermore, the powders have been examined (Neofytidis et al., 2015) as anode electrodes for their sulfur tolerance in the reaction of internal methane steam reforming, under high and low H₂O/CH₄ ratios, including 10 ppm H₂S. So far in these studies, using either helium diluted or real high concentration H₂O/CH₄ mixtures, the main conclusion was that the 3Au-3Mo-Ni/GDC sample proved to be the most sulfur and carbon tolerant electrode, compared to Ni/GDC and the binary 3Au-Ni/GDC and 3Mo-Ni/GDC. The superior performance of the ternary electrode was attributed to a synergistic interaction of the trimetallic Au-Mo-Ni solid solution that seems to modify Ni's catalytic properties and protect nickel against carbon and sulfur poisoning. In addition, a more conclusive and thorough discussion is presented regarding the

electrokinetics of the steam reforming reaction on the GDC and YSZ cermets paying considerable attention on the role of the support on the catalysis and electro-catalysis of the Ni based cermet electrodes.

KINETICS OF THE CH₄ STEAM REFORMING REACTION ON NI BASED CERMETS: THE CASE OF NI/YSZ

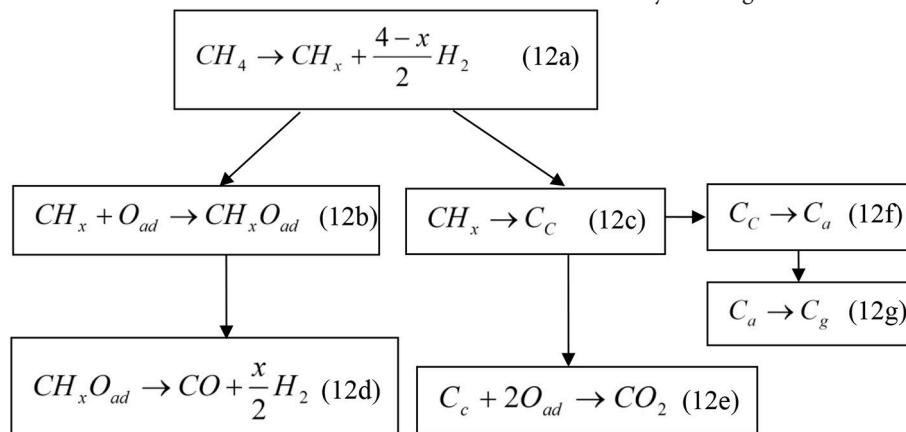
Beyond the general reaction scheme (1–4) depicted for the steam reforming and the water gas shift reactions the catalytic reaction steps involve the reactants' adsorption and surface reaction steps, which can determine both the rate and the selectivity of the whole process. The specific experimental evidences for the derivation of the proposed reaction mechanism are based on specific experiments carried out on Ni/YSZ. Nevertheless, though the support plays a major role on the kinetics of catalytic and electrocatalytic reactions, the general scheme proposed can be valid for both Ni/GDC and Ni/YSZ. Then, differences can be

by its reaction with the YSZ evolved oxygen at these elevated temperatures.

In addition to the TPSR experiment of **Figure 1** and far more interestingly the corresponding Temperature Programmed Oxidation (TPO) experiments depicted in **Figure 2** (Triantafyllopoulos and Neophytides, 2006) show that the main products for both samples are CO₂, CO, and H₂. CO₂ desorbs above 500 K, with the peak maximum at 600 K for Ni(Au 0.2 at%)/YSZ and 680 K for Ni(Au 1.0 at%)/YSZ.

The interest on the TPO experiments can be focused on the simultaneous evolution of CO and H₂ at essentially the same peak temperature maximum positioned around 700 K. This observation shows that CO and H₂ are products originating from the dissociation of the same compound, such as oxyhydrogenated carbon species (reaction **12d**), which are formed by the oxidation of the CH_x species with the preadsorbed O₂ (reaction **12b**). CO₂ is formed by the oxidation of carbidic species (reaction **12e**) (Triantafyllopoulos and Neophytides, 2003).

In this respect the following kinetic model has been proposed that describes the partial oxidation of methane toward the formation of synthesis gas:

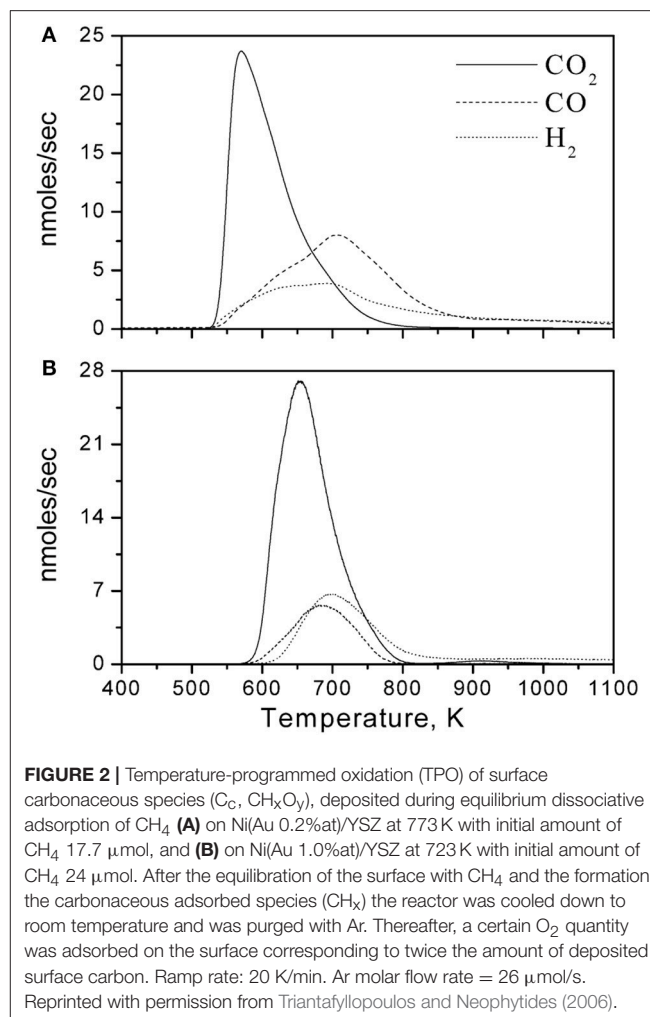
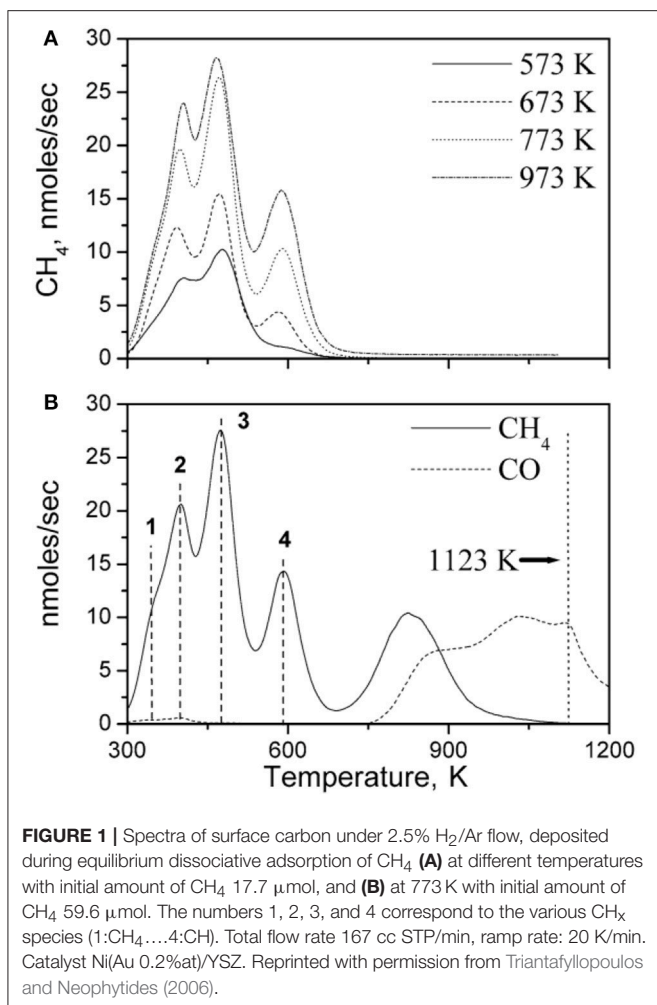


related to the activities of the various intermediate steps, which can be attributed to the effect of the support. This will be more obvious within the next sections, where the kinetics and electrokinetics of the ISR will be discussed.

The main carbon/carbonaceous species that drive CH₄ process are the various hydrogenated carbon species (CH_x) originating from the successive dehydrogenation of the CH₄ on the Ni surface, the active carbidic species C_c and the non-reactive graphitic species C_{gr}. These have been detected by means of Temperature Surface Reaction Spectroscopy by flowing H₂/Ar mixtures of the Ni based YSZ cermets (Triantafyllopoulos and Neophytides, 2006). Prior to this the various species were created on the surface by the equilibrium adsorption of certain aliquots of CH₄ on the catalytic surface at various temperatures. A typical TPSR experiment is depicted in **Figure 1** with the peaks within the temperature range of 300–600 K to be attributed to the various hydrogenated species (CH_x), while the peak at 800 K corresponds to adsorbed C_a species, which are considered as the transition species for the formation of graphitic C_{gr}.

The evidence of the existence of the latter is implied by the evolution of CO at the elevated temperatures >800 K originating

The reaction schemes (12a–12e) as written they represent the partial oxidation of methane to produce CO and H₂. Nevertheless, this can represent a general reaction scheme that can be valid in the steam reforming process as well as in the electrochemical partial oxidation of CH₄, which can take place in SOFCs. The source of the oxidic species that may participate in the oxidation reactions 12b or 12e can originate from the dissociative adsorption of water, thus processing the steam reforming reaction, or they can be supplied electrochemically as O²⁻ from the O²⁻ conducting solid electrolyte (YSZ), on which the Ni based electrode is supported. Reaction steps (12f) and (12g) show the route for the formation of adsorbed carbon species (C_a) and graphite (C_g) (Goodenough and Huang, 2007). C_a reacts both with H₂ and O₂ at higher temperatures (>800 K) than the carbidic C_c species (Goodenough and Huang, 2007). The formation of C_a is the precursor for the formation of the graphitic layer. The formation rates of C_a and C_g directly depend on the dissociation rate of the CH_x species and the nucleation rate of the C_a species, respectively. In addition the oxidation rate of the CH_x species into CH_xO_{ad} can determine in a decisive way the selectivity toward C_c, C_a, and C_{gr} and specifically



the selectivity toward CO₂ through reaction 12e. As has been shown in Triantafyllopoulos and Neophytides (2003), the fact that CO₂ is formed through a parallel process with respect to CO formation (reaction steps 12d and 12e respectively), involving complete dehydrogenation of CH₄ into C_c, the CO₂ selectivity can be an indicative criterion on the tendency of the catalyst to accumulate C_{gr}.

The transient experiment of **Figure 3** (Gavrielatos et al., 2008) confirms the significance of reaction step 12b and 12d for the production of CO and H₂ while bypassing the steps that lead to carbon formation. As depicted in **Figure 3** dry methane/Ar mixture (total flow ~100 cc/min with ~4.5 kPa CH₄) is initially introduced over a NiAu(5 at%)/YSZ anode. CH₄ reacts dissociatively with the Ni surface to form H₂ and apparently to form deposited carbon on the Ni surface. The open circuit potential was V_{OCp} = -1,486 mV. At time $t = 0$ a constant potential $V = -1,200$ mV is applied corresponding to a current density $i \approx 4.3$ mA/cm². Note that H₂ formation rate decreases by more than 50% accompanied by CO formation. No water or CO₂ formation was detected, thus confirming that the decrease in H₂ formation rate is due to the decrease of methane dehydrogenation rate. Thereafter H₂ formation rate

increases steadily to a steady state value that corresponds to the stoichiometry of the partial oxidation of methane according to reaction (11). The rates of reaction steps (12b) and (12c) and specifically the promotion of the oxidation step 12b and the inhibition of the C_a formation step 12c will determine the rate of the steam reforming or partial oxidation processes as well as the carbon formation of the process. Thus, it is expected that a carbon tolerant catalyst will catalyze the oxidation of the intermediate CH_x species faster than their sequential catalytic dehydrogenation toward C_a species formation. Thus, it appears that by applying a current the decrease in the rate of H₂ production implies that the sequential dehydrogenation of adsorbed methane hydrogenated species is disrupted by their oxidation due to the supply of O²⁻. This is further corroborated by the fact that after 1900s of current application, where the reaction rates reached steady state the production rate of H₂ and CO correspond to the selective processing of reaction (11), which is still 30% lower than the H₂ formation rate that corresponds to CH₄ dissociation at the open circuit ($I = 0$ no flux of O²⁻). The afore discussion shows that the reactions toward carbon formation are completely inhibited and as will be presented in

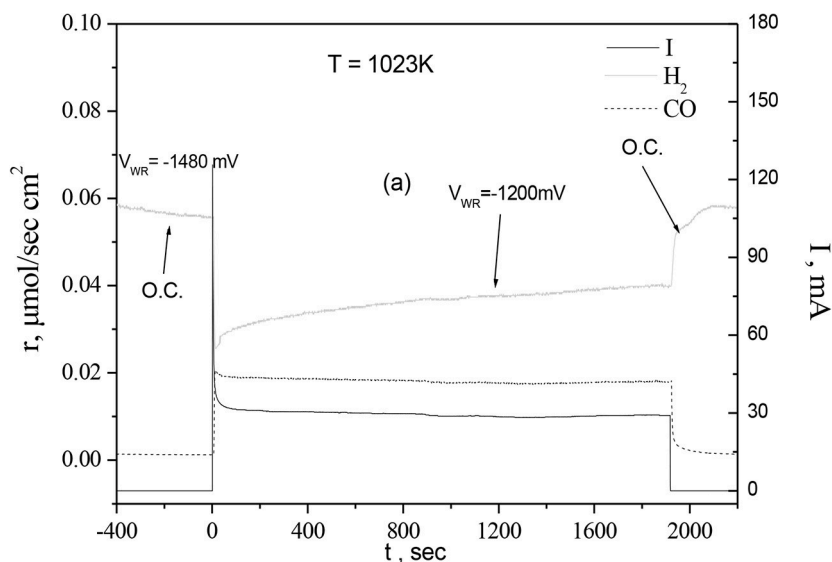


FIGURE 3 | Dynamic response of the production rate of H₂ and CO at T = 1,023 K) on NiAu5%at/YSZ upon constant voltage application. Reprinted with permission from Gavrielatos et al. (2008).

the next sections this is mainly attributed to the modification of Ni/YSZ catalytic and electrocatalytic properties by the atomically dispersed Au on the Ni surface.

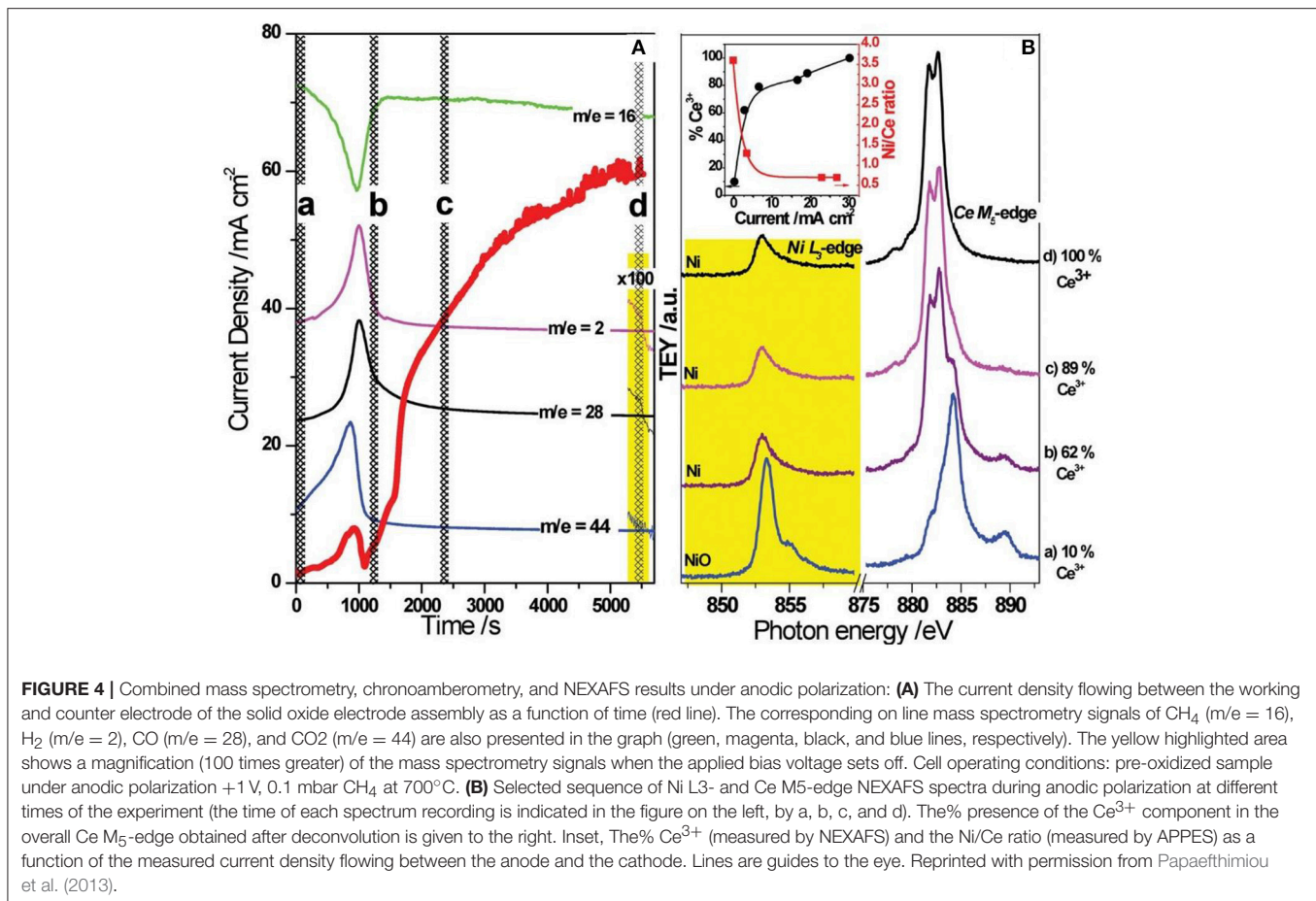
Last but not least the retarding of the dehydrogenation reactions can be also the result of the electrochemical promotion of the NiAu(5%at)/YSZ owing to the positive polarization and the increase of the work function of the catalytic surface. The latter can be corroborated by similar observation from European Fuel Cell Group IEA Advanced Fuel Cell Programme (1994) where significant non-faradaic decrease of the carbon deposition rate was observed during the steam reforming of methane upon polarization of the Ni/YSZ electrode. In addition in the case of Ni/GDC operating under S/C = 1 the supply of O²⁻ to the electrode induced around 25% decrease in the rate of the steam reforming reaction at current densities as high as 250 mA/cm² (Souentie et al., 2013). In general it was observed that the decrease in the steam reforming reaction rate was equal to the applied current onto the Ni/GDC electrode.

THE ROLE OF GDC IN CH₄ STEAM REFORMING AND PARTIAL OXIDATION PROCESSES

The dynamic nature of the Ni/GDC anode surface has been elucidated in Papaefthimiou et al. (2013) by the use of Ambient pressure X-ray photoelectron and near edge X-ray absorption fine structure spectroscopies (APPEs and NEXAFS respectively). These surface techniques are combined with on line electrochemical and gas phase measurements. The effect of the surface state on the electrocatalytic performance during direct methane electrooxidation was studied by performing transient chronoamperometric experiments over pre-oxidized Ni/GDC

anodes, biased to +1V under CH₄ atmosphere. In **Figure 4** the cell current and the gas phase composition are recorded with respect to the time evolution. The main features of Ni L₃- and Ce M₅-edge NEXAFS spectra that are being recorded during the evolution of the experiment and are depicted in **Figure 4**. In addition to the spectra evolution the inset of **Figure 4** depicts the relative concentration of the Ce³⁺ species with respect to the overall ceria spectrum (see Supporting Information S5 for details of Papaefthimiou et al., 2013). Initially and upon the application of the constant voltage +1V the anode is still largely oxidized with Ni and Ce being at 2+ and 4+ respectively (Ni²⁺, and mainly Ce⁴⁺), while the current flow is negligible. The reduction of Ni²⁺ to Ni⁰ is accompanied by the simultaneous decrease in CH₄ concentration and the production of oxidation products (H₂, CO, CO₂ but also H₂O and O₂, the latter not presented in the graph). Ni²⁺ reduction is accompanied by the increase in current due to the increase of the electrical conductivity of the electrode and the facilitation of the electrochemical reactions. The observed maximum in CO₂ formation rate coincides with the local maximum of the current at Time < 1,000 s, while the appearance of H₂ and CO after the maxima of current and CO₂ may imply partial oxidation of methane most probably accompanied by carbon deposition. The latter can be the cause for the transitory decrease in the current. The partial reduction of Ce⁴⁺ to Ce³⁺ (spectrum b) stimulates a notable increase in the current. It appears that the complete reduction of Ce⁴⁺ to Ce³⁺ induces a significant increase in current which can be even higher than an order of magnitude with respect to the initial maximum observed earlier.

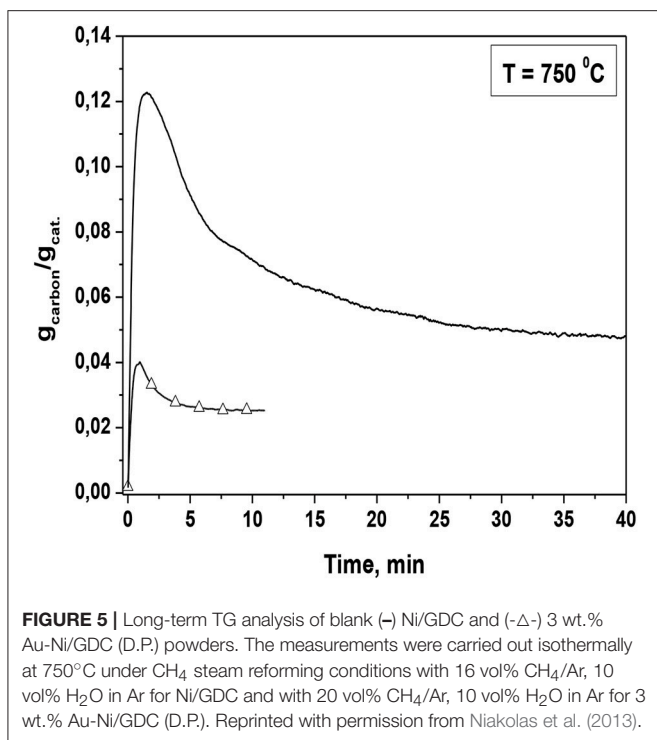
Note that the current increases in the process of Ce⁴⁺ reduction to Ce³⁺, followed by simultaneous surface enrichment in ceria.



The aforementioned experimental observations can be used in order to shed light on TGA experiments that were carried out under steam reforming conditions (Niakolas et al., 2013). As shown in **Figure 5** upon introducing S/C mixture consisting of 10 kPa H₂O and 20 kPa CH₄ the weight of the Ni/GDC catalyst increases initially with high slope indicating high carbon deposition rate. Within a time frame of 2–3 min the weight of the sample reaches a maximum and thereafter a gradual decrease is observed implying consumption of the deposited carbon until the weight stabilizes. This means that no further carbon accumulation is observed on the catalytic surface. In summary the TGA experiment of **Figure 5** shows a quite fast built up of carbon deposit, which is depleted thereafter down to zero deposition rate within a time frame of 40 min. The latter can be compared to the time evolution of the Ni/GDC activation of the APPES experiment depicted in **Figure 4**. Note that the decrease in the current observed after the local maximum at 1000s (**Figure 4**) can be related to deactivation owing to carbon deposition after the reduction of Ni surface. Thus, it can be inferred that the ability of Ni/GDC to oxidize deposited carbon is directly related to the partial reduction of Ce⁴⁺ to Ce³⁺, which presumably happens after the maximum reached in the weight of the catalyst (**Figure 5**). This can be attributed to the ability of the partially reduced ceria in the GDC composite to activate O.

The reactive O species can originate either by the activation of steam onto the GDC surface or the electrochemically supplied O²⁻ from the YSZ electrolyte. The latter has been proven in Papaefthimiou et al. (2013), both experimentally (APPES) and theoretically by the use of DFT calculations. Specifically during the course of the experiment depicted in **Figure 4** excess oxygen was observed owing to current application which did not correspond to the lattice oxygen of the partially reduced Ce³⁺. By means of DFT calculations it was calculated that the existence of this interfacial O causes the increase of the FERMI level of the Ni/GDC system, which can affect the rate of the dehydrogenation adsorption steps of methane on Ni so that it can be matched with the enhanced supply of the activated oxidic species from GDC aiming to the increase in the rate of reaction step 12b that leads to the formation of CO and H₂ so as to avoid the formation of carbon deposits through reaction steps 12c 12f, and 12g. In summary it proposed that the relatively high carbon tolerance of Ni/GDC cermet is mainly attributed to the ability of the partially reduced ceria to act as active catalyst support that activates interfacial O species, which become highly reactive with adsorbed CH_x so as to drive the CO and H₂ formation through the reactions 12b and 12d.

The role of CeO₂ as an active catalyst support has been vastly studied and its ability to induce strong metal support interactions



has been attributed to the enhanced oxygen mobility as well as the enhanced oxygen storage of CeO₂, which can exceed its chemical stoichiometry. Strategies to enhance these two properties of CeO₂ are being described in Li and Gong (2014), Konsolakis (2016) and comprise the insertion and substitution of Ce with another metal of similar size or different oxidation state. In the present case of gadolinium doped Ceria (GDC), the lower valence of Gd provides in addition the necessary O²⁻ conduction for the establishment of the effective electrochemical interface. The latter can induce strong modification of the catalytic properties of the supported metal particles through the effect of the Electrochemical Promotion in Catalysis (Vayenas et al., 2001). Furthermore, the interaction of the Ni species with CeO₂ can involve the insertion of Ni atoms in the lattice of CeO₂, which are not easily reducible, while as it has been proposed the dispersed Ni species are those experiencing the strong metal support interaction effect (Du et al., 2012). In consideration to the above discussion the participation of Ni species in the CeO₂ lattice can enhance the anchoring and stability of the finely dispersed Ni particles, as well as the oxygen mobility and storage of the Ni/Ce O₂ interface.

THE MODIFICATION OF Ni/YSZ AND Ni/GDC WITH Au AND Au-Mo ADDITIVES

Our attempts toward the increase of the carbon tolerance of the Ni/YSZ and Ni/GDC anodes were focused on their doping with small quantities of Au 3 wt% and Au3 wt%-Mo 3 wt%. The preparation of Au-Ni/YSZ was done by the use of the combustion synthesis method (Gavrielatos et al., 2008) directly onto the YSZ

electrolyte. In the case Au or Au-Mo on Ni/GDC the metals were deposited on the Ni/GDC powder by the use of the deposition precipitation method (Niakolas et al., 2013). The Au content in the samples was very close to the aforementioned nominal composition, while in the case of Mo the as prepared sample was 0.55 wt% and after the heat treatment of the electrode at 1100°C its amount was around 0.3 wt%. The lower loading is related to the preparation method, while the further decrease after the heat treatment can be attributed to the sublimation of Mo oxides. The samples were thoroughly characterized by means of XRD, XPS, and SEM before and after reduction. Characteristic temperature program reduction XRD (TPR-XRD) spectra are shown in **Figure 6**. The reduction of Ni/GDC cermet is initiated at 366°C and Au3-Ni/GDC starts at 370°C. This corresponds practically to the same reduction temperature for these two samples, while for the Au3-Mo30-Ni/GDC the reduction takes off at 539°C. Specifically, by comparing Ni/GDC and Au3-Ni/GDC XRD-TPR patterns after the reduction, the diffraction peak of Au is no longer detectable by XRD implying its possible absence as Au bulk crystal particles. A general observation is that in the ternary sample the evolution of the Au peak with increasing reduction temperature appears with larger shift strongly indicating the interaction with Mo species. In addition the peak of reduced Ni is broader with a significant 2θ shift (0.15°) with respect to the Ni peak of the non-impregnated sample. This unusual evolution of the Ni peak can be coupled with the aforementioned Au-Mo diffraction peak. The delayed reduction of NiO and the appearance of the shifted and broader nickel diffraction peak can be attributed to the Ni-Au-Mo solid solution formation.

Similar shifts in the XRD spectrum of Ni-Au supported catalysts are being described in Wu et al. (2013) and has been attributed to the formation of Ni-Au alloy.

The fine dispersion of the promoting species on the Ni surface during the reduction of Ni is verified by the XPS measurement depicted in **Figure 7**. It is clearly shown that Au signal is increasing significantly (>five times) upon Ni reduction indicating increase of the dispersion of the Ni particles, which in accordance to the XRD spectra, is processed through the dissolution of the Au particles in Ni. Chin et al. (2006) have reported that the XANES analysis of the Au-Ni/MgAl₂O₄ catalysts revealed the atomic distribution of Au atoms on the Ni surface and the transfer of electronic charge from Au to Ni as a result of surface alloy formation. In this respect it is relatively safe to consider that the catalytically exposed Ni surface is enriched with Au atoms thus inducing significant modifications in the electronic properties (Fermi level, work function, and d-band center) (Besenbacher et al., 1998) so as to affect the bonding strength of adsorbed species on the surface. Based on DFT calculations conducted by the group of Norskov et al. (Kan and Lee, 2010a) the d-band center of Ni shifts to higher potentials, which can presumably inhibit the dehydrogenation process on the Ni surface as it weakens the bonding strength and interaction of H adatoms with the Ni surface atoms.

The retarding of the CH₄ dehydrogenation process has been verified by measuring the activation energy of CH₄ dehydrogenation on Au modified Au-Ni/GDC powders. This was done by means of TGA isothermal experiments by measuring

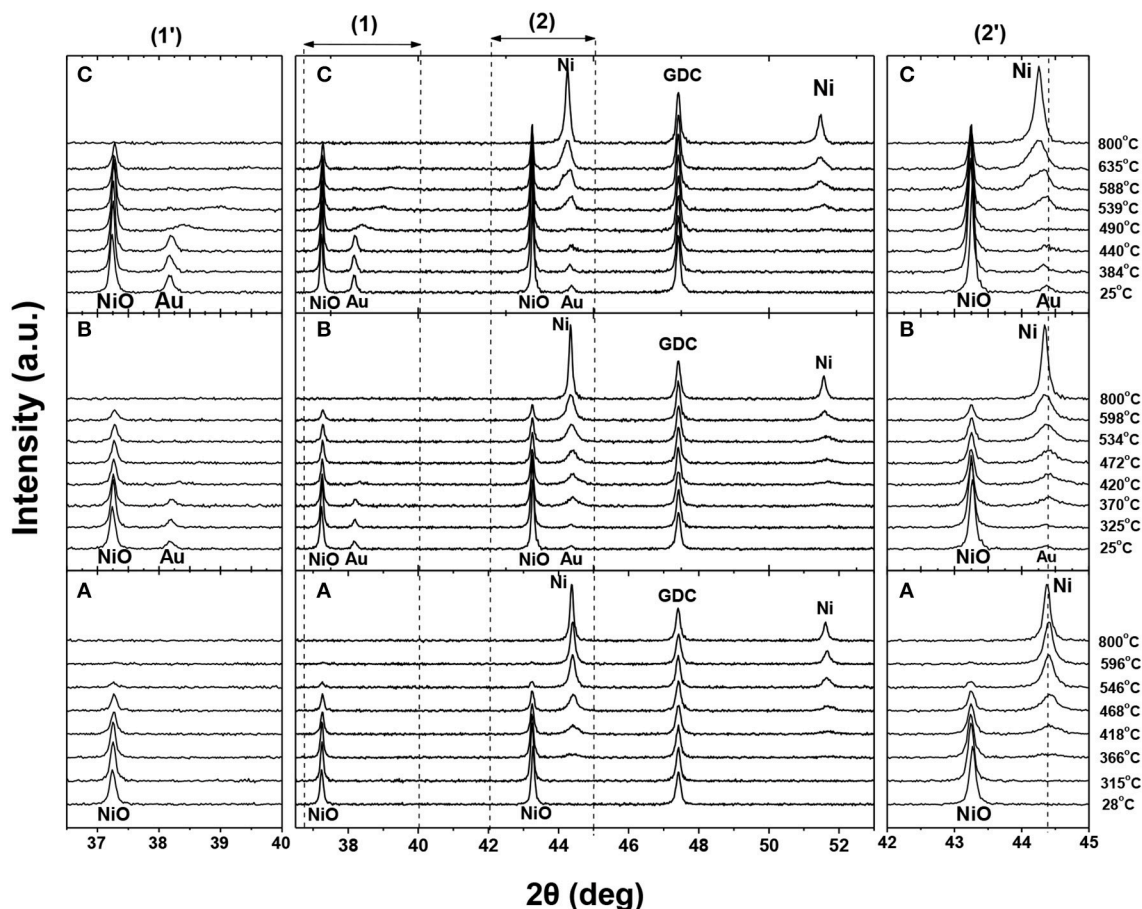


FIGURE 6 | XRD—TPR patterns of (A) blank Ni/GDC, (B) 3 wt.% Au-Ni/GDC (D.P.), and (C) 3 wt.% Au-30 wt.% Mo-Ni/GDC (D.CP). During the XRD analysis all samples were *in situ* reduced under 2 vol% H₂/N₂, while the temperature increased from 50 to 800°C at a rate of 5°C min⁻¹. The frames (1') and (2') depict the magnification of the dotted (1) and (2) areas. The labeled XRD peaks correspond to Au (JCPDS 04-0784), NiO (JCPDS 44-1159), GDC (JCPDS 46-0508), and Ni (JCPDS 04-0850). Reprinted with permission from Niakolas et al. (2013).

the rate increase of the sample's weight owing to the carbon deposits. The activation energy was increasing with increasing Au content and it was varied from 23 to 37 kcal/mol for various Au doping levels **Figure 8**.

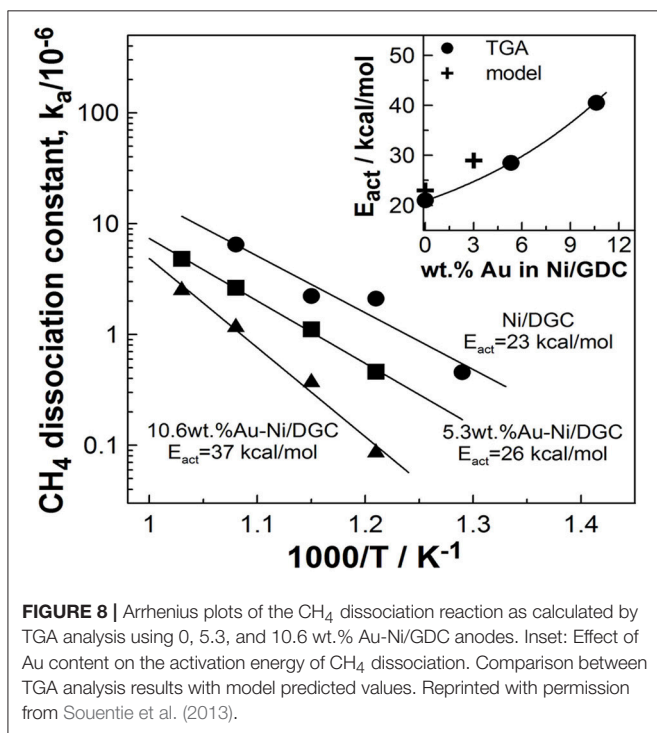
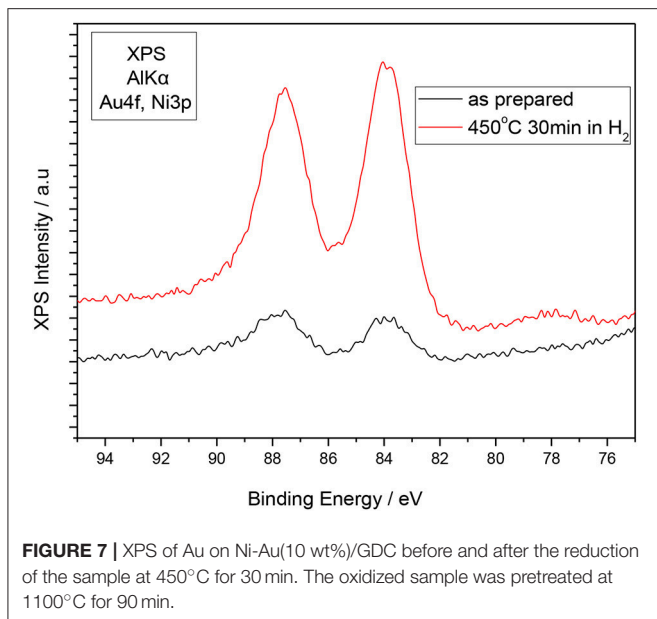
Far more interestingly as evidently shown in the SEM images in **Figure 9** by processing 1 kPa CH₄/N₂ over the Au-Ni/GDC or Au-Mo-Ni/GDC at 800°C no carbon deposits were observed. On the contrary in the case of Ni/GDC carbon whiskers have been developed even at this low CH₄ content (1 kPa) and for a reaction time of only 15 min.

ELECTROKINETICS AND CARBON TOLERANCE OF NiAu/YSZ ANODES UNDER STEAM REFORMING CONDITIONS

The electrochemical behavior of the Ni(Au 1 at%)/YSZ anode, prepared by the combustion synthesis method directly on the YSZ electrolyte, was studied by carrying out several electrochemical measurements under internal steam reforming

conditions at 1,123 K and different S/C ratios, ranging from 1 to 0.33.

Figure 10 depicts the effect of O²⁻ electrochemical flux on the rates of H₂, CO and CO₂ for S/C ratios 1, 0.5, and 0.31 respectively. At open circuit the steam reforming reaction produces H₂, CO and very small amount of CO₂. Under fuel cell operation, hydrogen, and carbon monoxide are electrochemically oxidized to produce water, carbon dioxide, and electricity. CH₄ conversion was between 10 and 15%, thus ensuring differential operation and mass transfer free kinetics. Limiting current is observed at higher S/C ratios because of H₂ starvation. In all cases the sum of the carbon oxides rate either remains constant (**Figure 10**) or slightly decreases (**Figures 10A,B**) with increasing current. This is a strong indication that CH₄ does not participate directly in the electrochemical oxidation process. This behavior can be realized through the competitive adsorption of steam and O²⁻ supplied on the Ni surface. The fact that O²⁻ supply to the NiAu/YSZ electrode appears to oxidize only H₂ and CO even at lean water steam conditions this strongly indicates that O₂⁻ do not participate in the oxidation process CH_x species to



CH_xO according to reaction step 12b. This implies that O₂⁻ may not be discharged and adsorbed on the Ni surface but instead they can be selectively reacting directly with H_{ad} and CO_{ad} at the electrochemical grain boundaries between the Ni and YSZ particles. On the contrary CH_x species are reacting with the oxygen species O_{ad} originating from the dissociative adsorption of steam on the rest surface area of the Ni particle. As it will be discussed further this is a characteristic kinetic behavior of the NiAu/YSZ electrocatalyst while in the case of Ni/GDC the

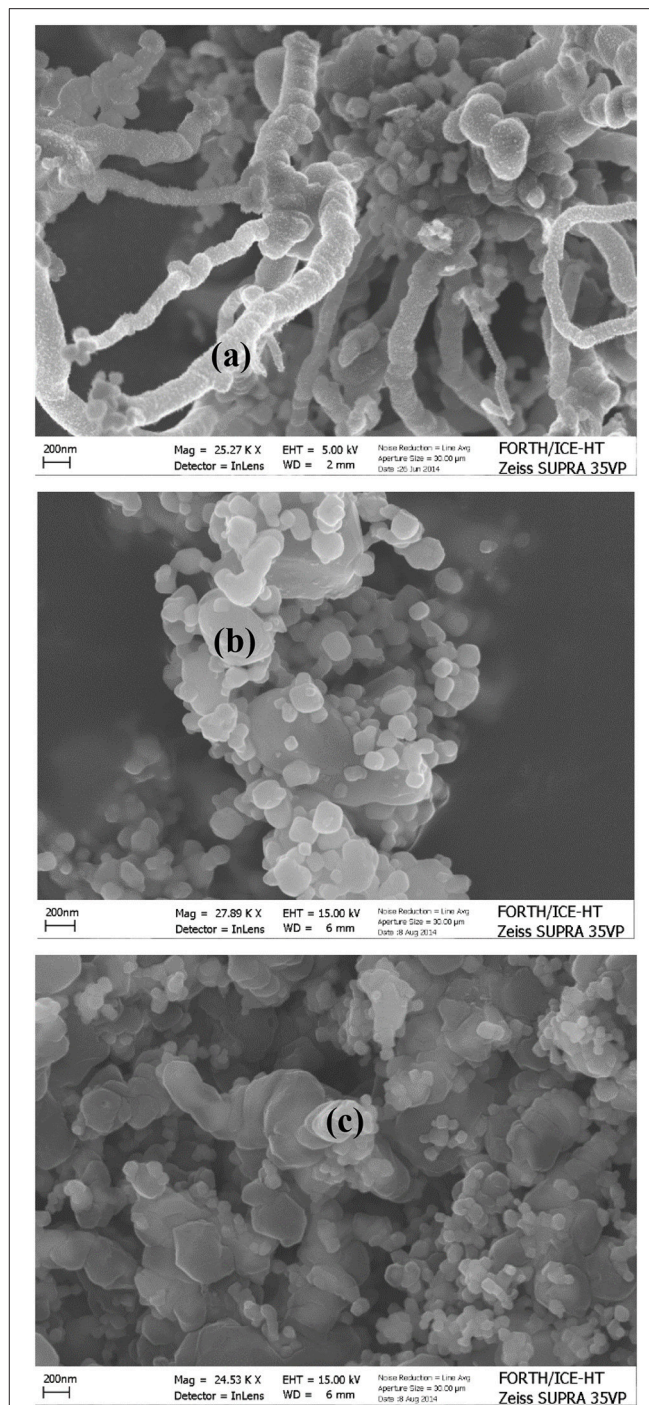
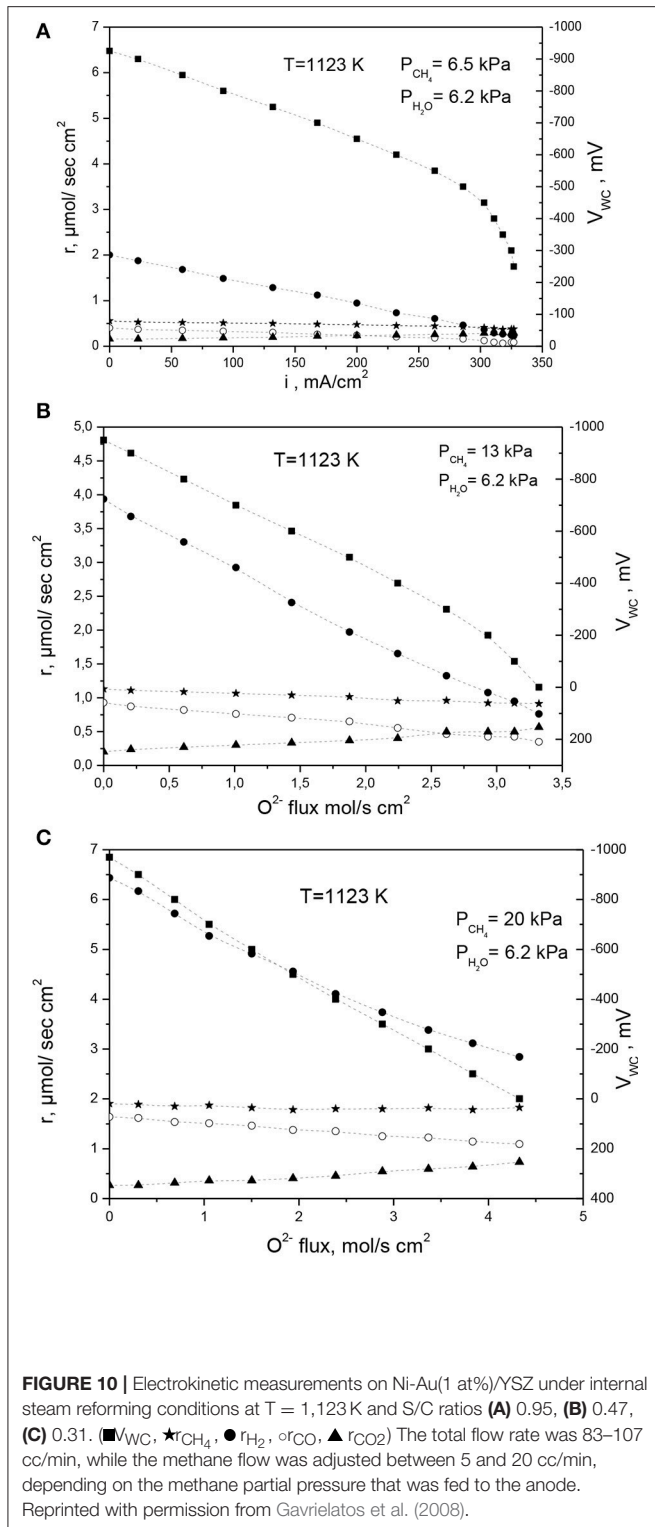


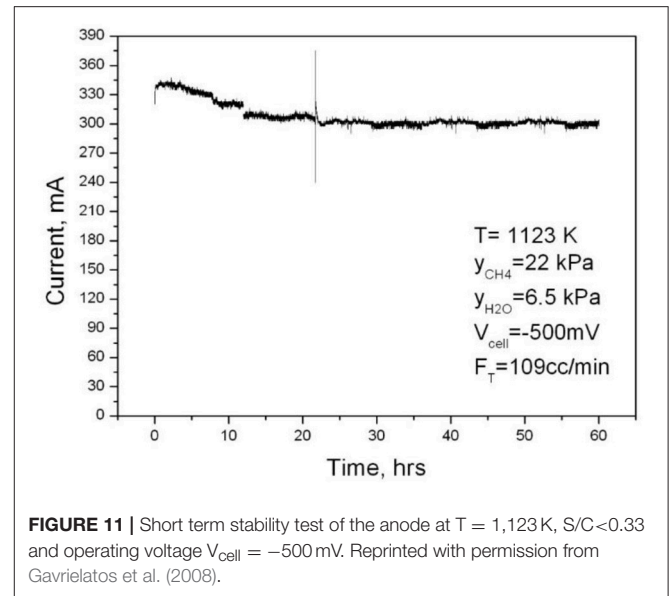
FIGURE 9 | SEM images after the *in situ* XRD with 1 vol.% CH₄/N₂ of: (A) Ni/GDC, (B) 3Au-Ni/GDC, (C) 3Au-3Mo-Ni/GDC. Reprinted with permission from Neofytidis et al. (in press).

electrokinetics of the reaction differ significantly thus denoting the specific role of the YSZ and GDC supporting particles.

The stability of the NiAu/YSZ electrode prepared with combustion synthesis was proven by the stability experiment depicted in **Figure 11**. The Ni(Au1 at%)/YSZ anode was fed



with water lean mixture containing ~ 22 kPa CH_4 and ~ 6 kPa water. The cathode was fed with Pure oxygen and the reactor was operating at 1,123 K and -500 mV (V_{cell}) producing about 300 mA/cm² for a time period of more than 60 h. Besides the small decrease in the current observed within the first 10 h

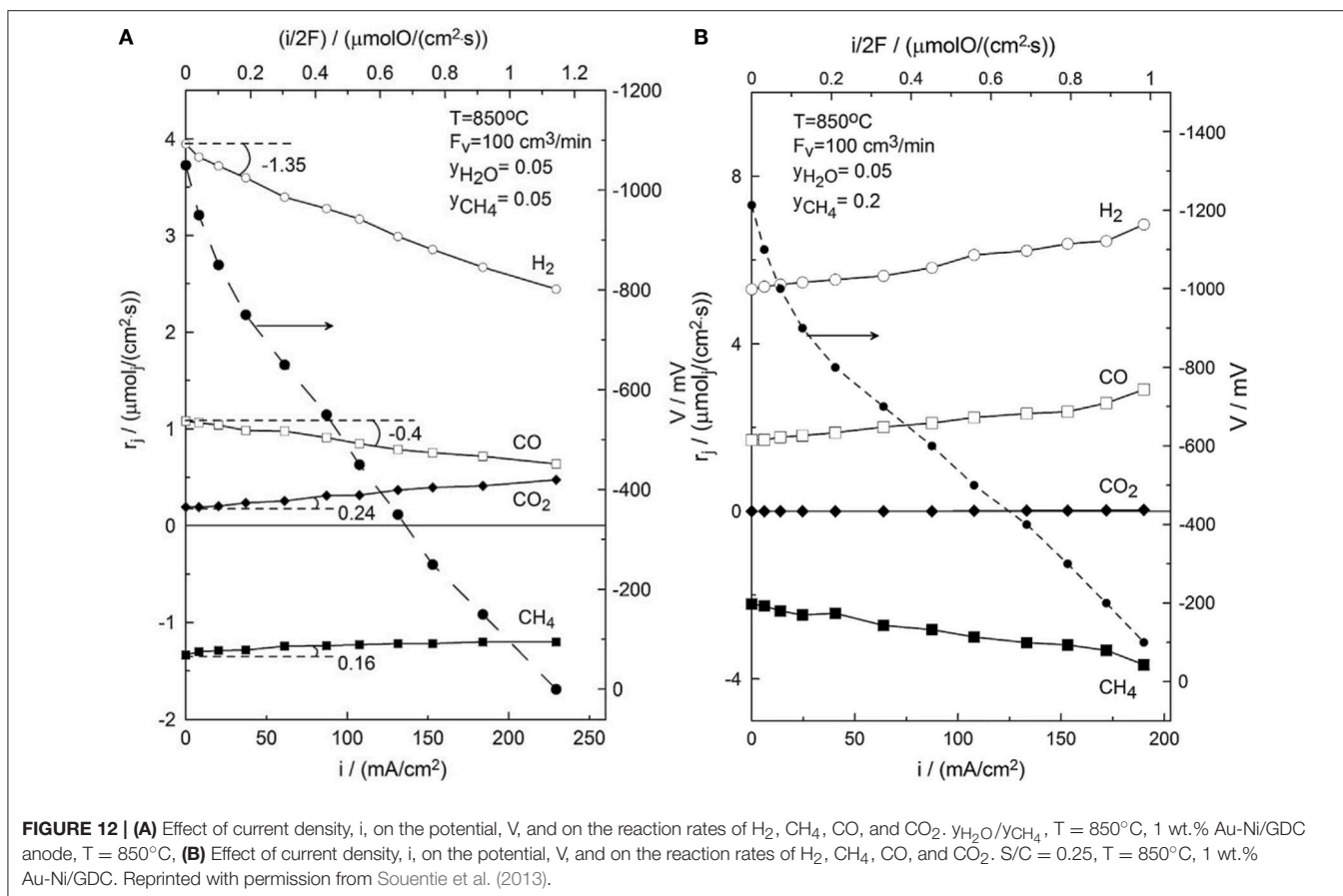


the performance of the reactor cell was fairly stable during the stability test. The electrochemical performance of the reactor cell under H_2 was the same, before and after the stability test. This further proves and confirms the high tolerance of the NiAu/YSZ electrocatalyst to carbon deposits, under internal steam reforming conditions.

ELECTROKINETICS AND CARBON TOLERANCE OF NIAU/GDC ANODES UNDER STEAM REFORMING CONDITIONS

The kinetic and electrokinetic behavior of the Ni/GDC and NiAu/GDC was studied under steam reforming conditions at S/C = 1 and 0.25. The electrokinetic behavior exhibits certain interesting features denoting the role of GDC both in the catalysis of steam reforming reaction and the electrocatalysis under S/C mixtures.

As it will be evidently shown this differs significantly from the corresponding behavior of NiAu/YSZ especially under current application. Of special interest is the behavior of the NiAu/GDC under lean steam conditions. **Figure 12** depicts the effect of electrochemical current application and O^{2-} supply on the evolution of CO and H_2 formation rates and on the rate of CH_4 consumption for S/C = 0.25, at $850^\circ C$. One observes that under open-circuit conditions, i.e., for $i = 0$, H_2 formation catalytic rate is a factor of three larger than the formation rate of CO, in agreement with the reaction stoichiometry. The mass balance of carbon based on the stoichiometry of the steam reforming reaction was satisfied. Interestingly under fuel cell operation conditions, the electrochemical formation rate of CO and H_2 increases linearly with current, accompanied by a linear increase in the CH_4 consumption rate, in contrast to the high S/C = 1 case, where by increasing current the consumption of CH_4 is slightly suppressed. Beyond the decrease in CH_4 consumption



rate the inhibiting effect of the applied current on the steam reforming reaction is also deduced by the fact that the sum of the slopes determining the CO and H_2 consumption rates is >1 that corresponds to the faradaic consumption of $H_2 + CO$. It is estimated that the rate of steam reforming reaction is decreased even up to 25% at the highest applied current density $I = 230 \text{ mA/cm}^2$ (Souentie et al., 2013). It is worth noting that no CO_2 formation rate is observed even under fuel cell operation conditions. Thus, in this case, it appears that the main anodic reaction is the partial oxidation of CH_4 (reaction 8) toward the formation of CO and H_2 .

This is a completely different behavior than the corresponding performance of the Ni/YSZ, where the electrochemical oxidation was limited to the oxidation of H_2 and CO only, formed by the steam reforming process. In the case of the GDC cermet the O^{2-} react in a quantitative way with the adsorbed hydrogenated carbonaceous species for the faradaic production of H_2 and CO . This behavior can be sought in the structure of the NiAu/YSZ and the NiAu/GDC cermets and the extend of the electrochemical interface between GDC or YSZ with Ni in relation to the size of Ni's catalytic surface area that is exposed to the reacting gases. The electrokinetic behavior of the NiAu/GDC implies that the size of the electrochemical interface is sufficiently high so as to provide access to the electrochemically supplied O^{2-} to the majority of the Ni surface. In this respect in accordance

to the transient experiment depicted in **Figure 3** the access of the electrochemically supplied oxygen to the majority of the Ni surface will facilitate its reaction with the CH_x species to produce CH_xO according to reaction 12b and thereafter its decomposition into CO and H_2 (reaction 12d). The ability of the Ni/GDC cermet to adjust its structure either exposing or encapsulating Ni has been studied and specified by the APPEX XPS and EXAFS experiments depicted in **Figure 13**. As it is explicitly shown maximum performance can be achieved at intermediate exposures of Ni and GDC at Ni/Ce around 0.4.

The structural modification of the Ni/GDC electrode is related to the exposure of the electrode to an oxidative or reductive atmosphere. In the extreme cases where the electrode is oxidized NiO is accumulated on the surface thus screening GDC, while at highly reductive atmospheres the metallic Ni particles are encapsulated by the GDC (Papaefthimiou et al., 2013).

The Stability of Ni-Au1.5 at%/GDC electrode is shown in **Figure 14** (line 1). This is compared to the performance of the blank cell (line 2) in **Figure 14** (Pujare et al., 1987). The stability experiment was carried out galvanostatically applying 500 mA cm^{-2} , while using several fuel streams. During the time periods (1a) and (2a), under H_2 operation, Au-Ni/GDC anode is performing better with higher cell voltage because of the lower ohmic losses of the former. Upon introduction of S/C mixture 3/2 the performance is slightly improved (period 1b), while

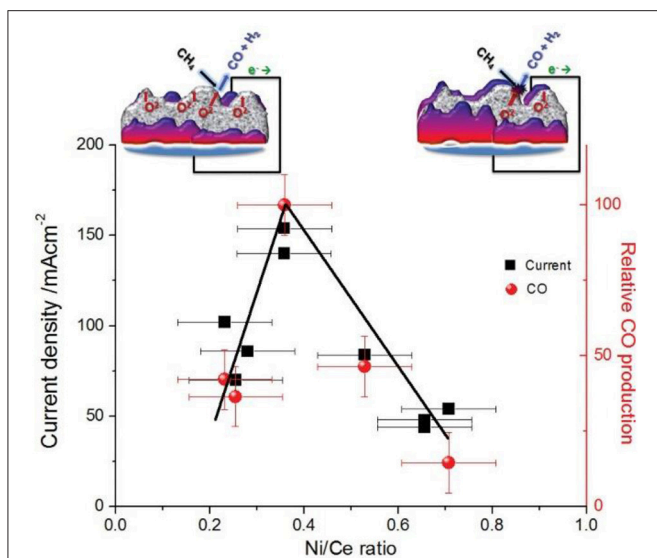


FIGURE 13 | Current and CO production as a function of surface composition. The current flowing at the SOEA (left y-axis) and the relative carbon monoxide production (right y-axis) as a function of the Ni/Ce ratio measured by *in situ* APPEs. Measurements are performed on samples with identical nominal composition, but subjected to different pretreatments in the cell prior to the measurements. In all cases ceria and nickel exist exclusively in the Ce^{3+} and Ni^0 oxidation states. The error bars represent estimated uncertainty based on the photoelectron peak area and mass spectrometry signal calculations. Lines serve as guides to the eye. *Conditions*: anodic polarization (+1 V), atmosphere: 0.1 mbar CH_4 , temperature: 700°C . The schematic shows the proposed surface arrangement in the case of a low (left) and a high (right) Ni/Ce ratio (ceria in gray and nickel in purple color). Reprinted with permission from Vorontsov et al. (2008).

by introducing reformat H_2 the cell voltage decreases (**period 1c**). This strongly indicates that the adsorbed CH_4 carbonaceous species (CH_x) are electrochemically even more active than H_2 species. By introducing lean steam to CH_4 mixture ($\text{S/C} = 1/2$, **period 1d**) the cell voltage increases further to 800 mV. In general it can be concluded that the electrocatalytic activity during the transition from hydrogen operation (**period 1a**) to internal steam reforming operation (**period 1d**) remains constant or it is even improved with respect to reformat gas operation. In particular, the performance of the cell is stable even under highly rich CH_4 conditions (**periods 1d** and **1e**) with a power density of 0.41 Wcm^{-2} at 810 mV.

On the contrary, a mirror image is observed in the case of the non-modified Ni/GDC experiment. The transition from H_2 feed (**2a**) to S/C mixture 3/2 (**2b**) results into a large decrease of the cell voltage and performance (even up to 100 mV). Notably, upon changing the S/C ratio from 3/2 (**period 2b**, **Figure 14**) to 1/2 (**period 2c**, **Figure 14**) the performance is progressively becoming worse with degradation rate of 0.3 mV/h. It is worth mentioning that the open circuit potential (OCP) on the Au doped anode is by 150 mV higher than that of the non-modified electrode under steam reforming. Note that the corresponding OCP under H_2 is the same for both cells.

As it is explicitly stated in Pujare et al. (1987) the higher OCP value in SOFCs implies a lower O_{ads} coverage on the anode

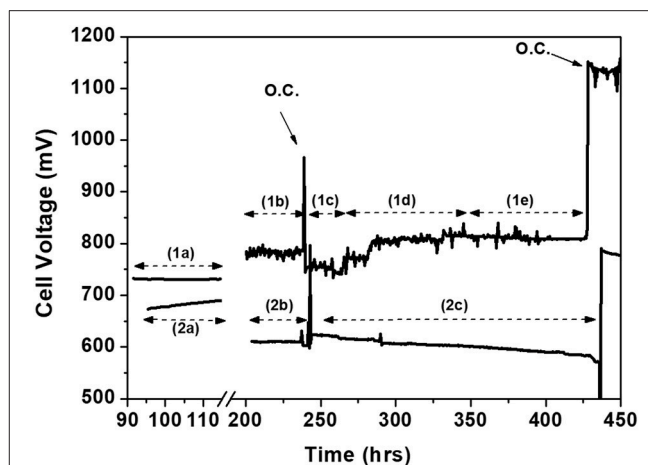
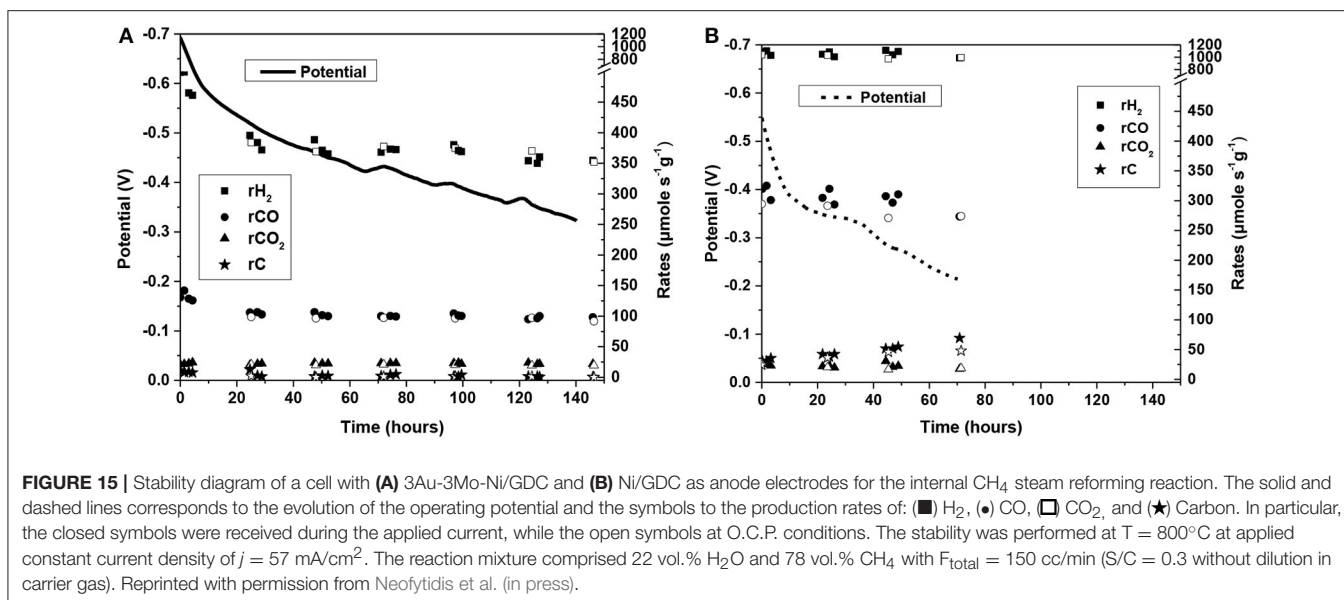


FIGURE 14 | Stability test diagram of two cells comprising 1.5 at% Au-Ni/GDC and Ni/GDC as anodes at $T = 850^\circ\text{C}$ and 500 mAcm^{-2} . Label **1** corresponds to the performance of the cell with the Au-modified anode and label **2** to the blank cell. *Conditions*: (**1a**) H_2 -3% H_2O $F_{\text{anode}} = 520 \text{ ccmin}^{-1}$, (**1b**) $\text{S/C} \approx 3/2$: $P_{\text{H}_2\text{O}} = 60.2 \text{ kPa}$, $P_{\text{CH}_4} = 41.2 \text{ kPa}$, $F_{\text{anode}} = 224 \text{ ccmin}^{-1}$, (**1c**) reformat feed: 77 vol.% H_2 , 8 vol.% CO , and 15 vol.% H_2O , $F_{\text{anode}} = 374 \text{ ccmin}^{-1}$, (**1d**) $\text{S/C} \approx 1/2$: $P_{\text{H}_2\text{O}} = 33.0 \text{ kPa}$, $P_{\text{CH}_4} = 68.3 \text{ kPa}$, $F_{\text{anode}} = 135 \text{ ccmin}^{-1}$, (**1e**) dry CH_4 feed, $F_{\text{anode}} = 90 \text{ ccmin}^{-1}$. (**2a**) H_2 -3% H_2O $F_{\text{anode}} = 856 \text{ ccmin}^{-1}$, (**2b**) $\text{S/C} \approx 3/2$: $P_{\text{H}_2\text{O}} = 60.1 \text{ kPa}$, $P_{\text{CH}_4} = 41.2 \text{ kPa}$, $F_{\text{anode}} = 509 \text{ ccmin}^{-1}$, and (**2c**) $\text{S/C} \approx 1/2$: $P_{\text{H}_2\text{O}} = 33.2 \text{ kPa}$, $P_{\text{CH}_4} = 68.1 \text{ kPa}$, $F_{\text{anode}} = 308 \text{ ccmin}^{-1}$. Reprinted with permission from Niakolas et al. (2010).

electrode. This can be attributed to the more reactive catalytic surface of the Ni-Au/GDC anode with the CH_x species indicating a promotional effect for reaction step **12b**.

ELECTROCATALYTIC STABILITY OF Ni-Au-Mo/GDC

The electrocatalytic stability of the ternary AuMoNi/GDC anode in comparison to Ni/GDC was studied under harsh steam reforming conditions by the use of highly concentrated CH_4 mixtures and $\text{S/C} \sim 0.3$ (Neofytidis et al., in press). In this respect in these experiments 30 kPa H_2O and 70 kPa CH_4 was used to carry out stability tests of the above samples. The stability curves in **Figure 15** show the comparison of the electrocatalytic performance between Ni/GDC and 3Au-3Mo-Ni/GDC, as electrodes in electrolyte-supported cells. The active functional layer was directly deposited on the YSZ electrolyte and the current collection was facilitated through a Ni mesh. The measurements took place in galvanostatic mode with an applied constant current density of 57 mA/cm^2 . The comparison includes the evolution of the operating potential over time, in combination with the catalytic production rates of H_2 , CO , CO_2 , and carbon. The latter rate has been calculated, like in the half cell measurements, by using the following mass balance expression of carbon (Equation 1). This expression is always valid under both O.C.P. and fuel cell operation conditions, where specifically the contribution of the applied current is also considered (Souentie et al., 2013):



$$r_{\text{H}_2} + \frac{I}{nF} = 3r_{\text{CO}} + 4r_{\text{CO}_2} + 2r_{\text{Carbon}} \quad (12)$$

where: I is the applied current, $n = 2$ is the number of the participating electrons and F is the Faraday constant.

The first observation is that the cell with the ternary electrode operated for 140 h, which is the double time-period than that of the cell with Ni/GDC (70 h). Specifically, the operating potential of the ternary 3Au-3Mo-Ni/GDC cell started from 692 mV and exhibited a total degradation rate of 2.6 mV/h. In the case of the cell with Ni/GDC, the operating potential started from a lower value (578 mV) and it degraded with a rate of 5.5 mV/h, which is almost two times higher than that of the ternary electrode.

The ternary electrode was catalytically less active for the studied reaction, having ~ 3 times lower production rates of H₂ and CO. Moreover, both electrodes showed almost similar production rates of CO₂. The key difference lies on the carbon formation rate and its evolution during the stability experiment. Specifically, the cell with 3Au-3Mo-Ni/GDC exhibited significantly lower to almost zero rate in the whole duration of the test (140 h). On the contrary, the cell with Ni/GDC had a measurable carbon formation rate from the beginning of the stability, which increased gradually during the course of the measurement. This is also confirmed by comparing, in **Figure 16**, the evolution of the selectivity to carbon formation for the two electrodes. The latter is expressed as the % ratio of the carbon formation rate (r_{C}) to the consumption rate of methane (r_{CH_4}), where $r_{\text{CH}_4} = r_{\text{CO}} + r_{\text{CO}_2} + r_{\text{C}}$. It is shown that in the case of the cell with Ni/GDC the selectivity to carbon was higher ($\sim 9\%$) from the beginning of the electrocatalytic measurement and during the stability it gradually increased to values close to 20%. On the other hand, the 3Au-3Mo-Ni/GDC anode showed less selectivity to carbon, starting from 5% that progressively decreased to values close to zero. Thus, it can be concluded safely that indeed the Au-Mo-Ni/GDC electrode inhibits the CH₄ decomposition toward C deposits [reaction (4)] and far more

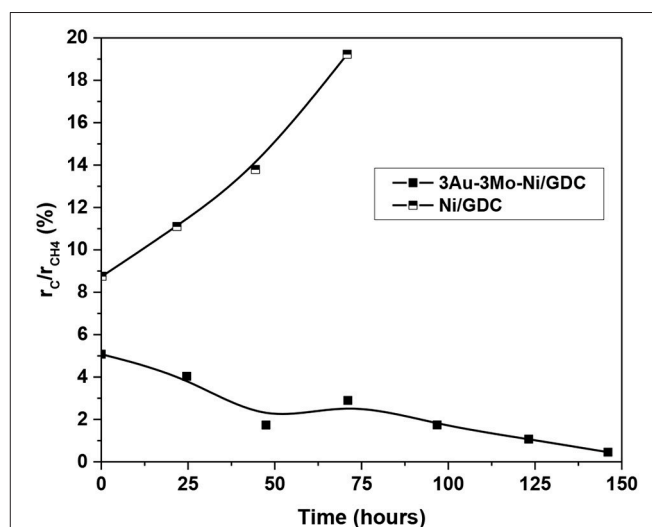


FIGURE 16 | Evolution of the % selectivity to carbon formation, for the examined cells with 3Au-3Mo-Ni/GDC (■) and Ni/GDC (●) anodes. Selectivity is expressed as the % ratio of the carbon formation rate (r_{C}) to the consumption rate of methane (r_{CH_4}), where $r_{\text{CH}_4} = r_{\text{CO}} + r_{\text{CO}_2} + r_{\text{C}}$. Reprinted with permission from Neofytidis et al. (in press).

interestingly the latter appears to be enhanced with increasing time on Ni/GDC, while it decreases down to almost zero on the Au-Mo-Ni/GDC anode without any loss in the catalytic reforming activity. This can be most probably attributed to the continuous improvement of the Au-Mo-Ni/GDC properties against carbon deposition, owing to the better distribution and structural positioning of the Au and Mo dopants in Ni (Niakolas et al., 2013; Neofytidis et al., 2015) and especially on the catalytic surface. The last observations point that part of the enhanced catalytic performance of the Ni/GDC electrode, especially for the production of H₂, can also be attributed to its higher catalytic

activity for the decomposition of CH₄ [reaction (4) or reaction 12a and 12c], which is mainly responsible for the formation of carbon deposits.

The decrease in the catalytic activity of the 3Au-3Mo-Ni/GDC sample with respect to the non-modified Ni/GDC is in accord with the d-band center theory proposed by Norskov et al. (Kratzer et al., 1996; Nørskov et al., 2011) and specifically dealing with the dissociation and dehydrogenation of CH₄ on the Au doped Ni surface. They proposed that the rate of CH₄ dehydrogenation will be retarded on the Au modified surface, due to the fact that the center of the d-band density of states shifts to lower energy below the Fermi level with respect to Ni. This renders the interaction of CH₄ and the successive dehydrogenation of the adsorbed CH_x species with the Ni surface weaker so that the rate of dehydrogenation slows down. Similar trend can be considered for the case of 3Au-3Mo-Ni/GDC, which is also corroborated by the fact that the 2θ shift of the Ni peak at 44.38° to lower 2θ is even larger than the corresponding peak of Au-Ni (Figure 6). In addition, it can be assumed that the bonding strength of the oxidic species, resulting from the dissociative adsorption of water during the course of the steam reforming reaction, is also weaker so as to be more reactive and drive the surface reaction step 12b faster, thus avoiding the complete dehydrogenation and carbonization reactions of the Ni surface. It must be noted that although steam reforming reaction rate on 3Au-3Mo-Ni/GDC is by factor of three lower than the corresponding rate on Ni/GDC, this is not expected to affect the operation of the electrode as the catalytic rate for H₂ production is still higher than the hydrogen demand to be electrochemically oxidized in the fuel cell.

Figure 17 shows the comparison of the impedance spectra for the cell with 3Au-3Mo-Ni/GDC and that with Ni/GDC anode, respectively. The EIS analysis started from the beginning of the stability test (t_0) and continued at specific time periods up to the end of the experiments.

The first comment is that in both cells the R_{ohm} and R_{pol} values are relatively high. This is mainly due to the cells' configuration and specifically to: (i) the thick electrolyte (300 μm) and (ii) the fact that the anode electrode comprises only the studied functional layer, without other layers (e.g., adhesion and/or current collection layer) that could decrease the R_{ohm} and R_{pol} values. Furthermore, the cells had a two electrode (working and counter) configuration, which means that the impedance spectra contain information from both electrodes. However, the reaction conditions on the O₂ (counter) side remained constant and the cells were prepared identically. Thus, the configuration of the cells does not hinder the purposes of this investigation and the observed variations of the resistances over time can be mainly ascribed to the induced changes on the examined anode (working) functional layers.

Specifically, at the beginning of the stability (t_0) the cell with the ternary electrode (Figure 17A) exhibited lower R_{ohm} and R_{pol} values, compared to the cell with Ni/GDC. This has been attributed to the different structural properties of the ternary electrode, induced by the formation of the Au-Mo-Ni solid solution. Indicatively, there is improvement on both the electron conductivity properties and the electrochemical

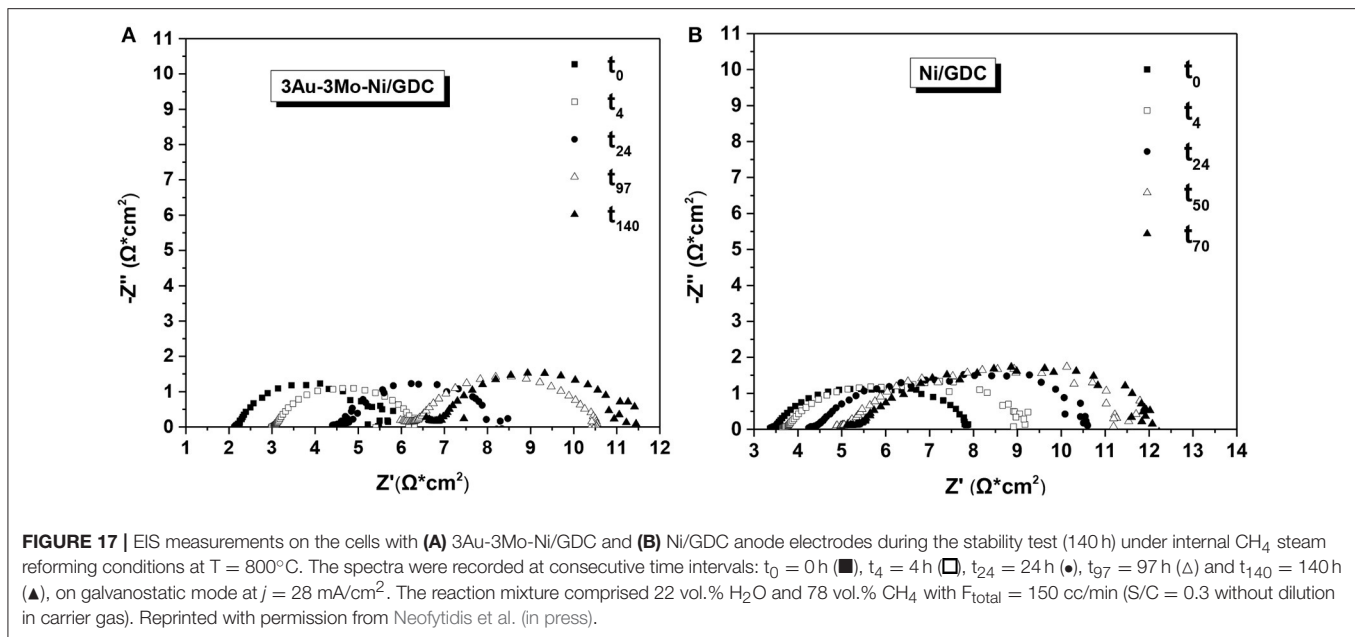
interface, developed between the Au-Mo-Ni and the GDC within the structure of the electrode, providing lower R_{ohm} and R_{pol} , respectively. Further investigation on this issue is currently in the progress, focusing on the changes of the bulk and the surface state of the electrodes, by applying HR-TEM and *in situ* H₂-XPS measurements.

During the evolution of the stability measurements, in the case of Ni/GDC (Figure 17B) the R_{pol} value increased significantly and this can be correlated to the gradual increase of the carbon formation rate. The accumulation of carbon deposits has been reported (Koh et al., 2002; Subotić et al., 2016a,b) that may block the pores of the electrode and the electrochemical interface at the three phase boundaries. As a result the gas fuel transport/diffusion is limited and there is inhibition of the chemical and electrochemical reactions on the anode side, causing the degradation of the operating potential. The R_{ohm} values exhibited also an increase, but at lower extent than that of R_{pol} , and the possible reasons are discussed in the next paragraphs.

In the case of the ternary electrode (Figure 17A) the EIS analysis showed a different behavior. The stability conditions had a minor effect on the degradation of R_{pol} , which did not increase significantly despite the longer (140 h) operation. This is in line with the fact that almost minimal carbon deposits rates were measured during the stability experiment. On the other hand, R_{ohm} was more affected and gradually increased, reaching slightly higher values than those of the Ni/GDC anode. Consequently, the degradation of the operating potential in the cell with 3Au-3Mo-Ni/GDC is mainly related to the increase of the ohmic resistance. This trend can be attributed (Koh et al., 2002; Matsui et al., 2007, 2010; Mogensen et al., 2011; Niakolas, 2014) to the possible gradual re-oxidation and/or agglomeration of nickel, due to the high partial pressure of H₂O in the reaction mixture.

In fact the direct comparison of Figures 14, 15 indicates that Au-Ni/GDC sample is superior to the 3Au-3Mo-Ni/GDC, due to the fact that essentially no degradation was observed on the former for a longer testing period. However, as already mentioned, the two electrodes cannot be compared directly because the electrode structure used in Figure 14 comprises the GDC adhesion layer, the Au-Ni/GDC functional layer and the Ni layer over the functional layer that is acting as a current collector. In addition, the current collector was a gold plated Ni mesh. In this respect the ohmic resistances of the anode functional layer of Figure 14 have been diminished, while in the case of the experiment of Figure 15 as has been revealed by the impedance spectra of Figure 17 the contact ohmic losses are comparable with the polarization resistance and especially for the case of 3Au-3Mo-Ni/GDC this appears to be the main cause of the degradation mechanism. Last but not least, note that the experiments of Figure 15 were carried out under S/C = 0.3, which is more difficult to process than the S/C = 2 conditions of the experiment of Figure 14.

In conclusion the cell with 3Au-3Mo-Ni/GDC exhibited higher performance from (t_0) up to the final measurement at ($t_{140 h}$). On the other hand, the higher carbon deposition rate of the cell with Ni/GDC affected as well the I-V plots (Neofytidis et al., in press), which exhibited lower performance from the



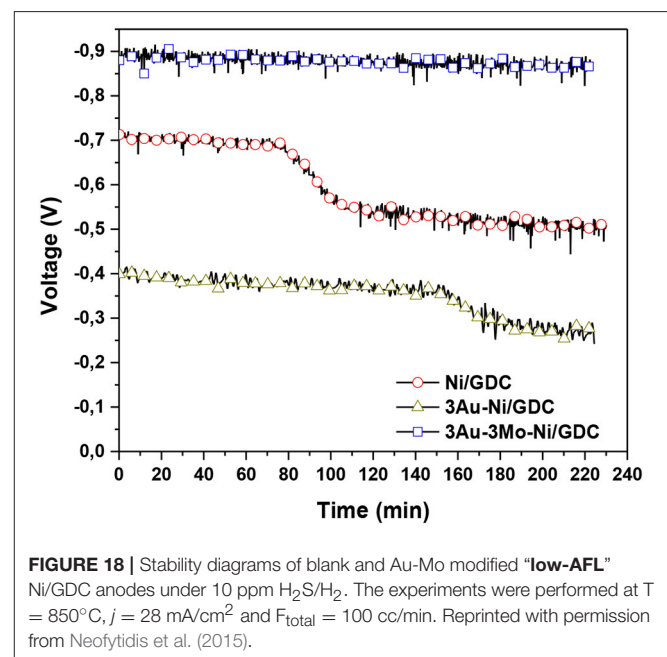
beginning of the stability and enhanced degradation up to the completion of the experiment at (t_{70 h}).

SULFUR TOLERANCE OF THE Ni/GDC, NiAu/GDC, AND NiAuMo/GDC

In Neofytidis et al. (2015) the effect of Au and/or Mo addition is presented and discussed with regards to the behavior and stability of the modified Ni/GDC electrodes in the presence of H₂S. In particular, it is shown that the Au-Mo-Ni/GDC electrode has the best and most stable performance both in the presence of 10 ppm H₂S under 100 vol% of H₂ in the feed under CH₄ and H₂O (in Helium) at S/C = 2 or S/C = 0.13.

Figure 18 shows the performance of the various Ni/GDC and modified anodes in the presence of 10 ppm H₂S/H₂ mixtures at 850°C. Ni/GDC and 3Au-Ni/GDC exhibited lower performance compared to the 3Au-3Mo-Ni/GDC, while they also presented a certain degree of degradation in the cell voltage after some time of exposure. In particular in both materials a step decrease in the cell voltage is observed after 70 min (Ni/GDC) and 160 min (Ni-Au/GDC). This step change can be related to the saturation of electrocatalytically active sites by the irreversible adsorption of S_{ad} species. The observed difference in the elapsed time period for the appearance of the voltage step decrease and the corresponding size of the voltage step change can be attributed to the effect on the S_{ad} deposition rate as well as on the equilibrium coverage of S_{ad} on these sites. In this respect the Ni-Au/GDC appears to be improved with respect to the non-modified Ni/GDC. However, 3Au-Ni/GDC anode showed the lowest cell voltage at the beginning of the stability while Ni/GDC showed a medium performance.

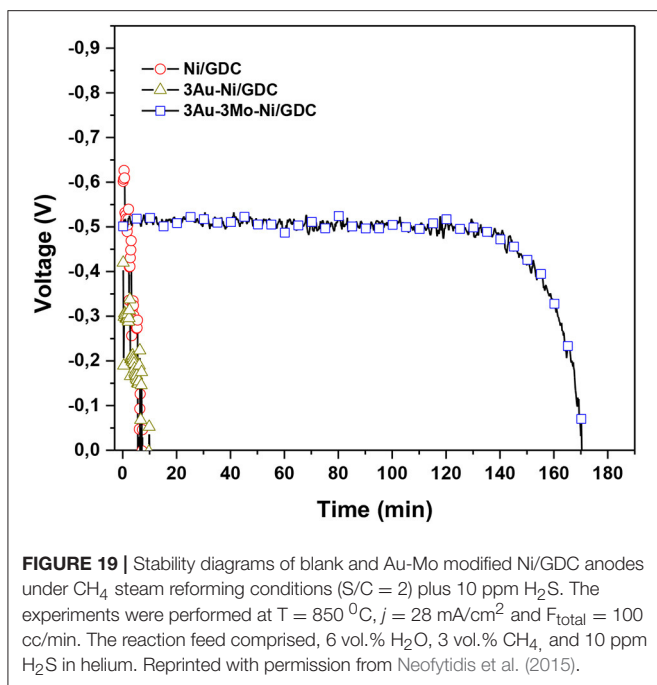
Interestingly the cell with the 3Au-3Mo-Ni/GDC anode exhibits quite stable performance within the examined time



period. The cell voltage was close to the corresponding voltage under H₂ flow without H₂S in the feed, thus yielding the higher current density.

Under internal CH₄ steam reforming conditions with the ratio S/C = 2 plus 10 ppm H₂S (**Figure 19**) the 3Au-3Mo-Ni/GDC electrode lasted for almost 2.5 h while the other two electrode materials had experienced a fast degradation reaching to complete deactivation within a time period less than 10 min.

The main difference of the operation under steam reforming conditions with respect to the use of H₂ as fuel is that in the



former case the poisoning effect of S is initially affecting the catalysis of the steam reforming reaction. In this respect the H_2 production is diminished, thus affecting severely the electrocatalytic performance due to H_2 fuel starvation.

As it is mentioned in Weaver and Winnick (1989) the Au-Mo-Ni/GDC is characterized by the following improved properties like (i) better electronic conductivity, (ii) better electrochemical interface between the electrode and the electrolyte, and (iii) enhancement of the electrocatalyst's sulfur tolerance. The longer life time of the Au-Mo-Ni/GDC can be attributed to the modification of the S bond strength with the catalytic surface so as to cause either the shift of the H_2S dissociation equilibrium to the left (decrease of the equilibrium constant) or/and concomitantly affect the rate of the dissociation reaction. These two processes can increase the life span of the catalyst since the rate of formation of the adsorbed S_{ad} species is retarded, thus elongating the time needed to cover and poison the catalytically active sites with S_{ad} .

Although, this synergistic interaction between Au-Mo-Ni is not enough to fully protect the electrode, however it can be sufficient for the protection of the electrode against peak increments in H_2S concentration.

In addition to the modification of surface adsorption properties of Ni, significant sulfur tolerance resistance can be obtained by modifying the ionic oxide support e.g., CeO_2 or the use of other mixed ionic/electronic perovskite materials like $\text{BaZr}_{0.1}\text{Ce}_{0.7}\text{Y}_{0.2-x}\text{Yb}_x\text{O}_{3-\delta}$ (BZCY_{Yb}) or $\text{BaZr}_{0.4}\text{Ce}_{0.4}\text{Y}_{0.2}\text{O}_{3-\delta}$ (BZCY), which can be oxygen ion or proton conductors (Wang et al., 2014; Chen et al., 2016). As for the case of carbon tolerance, CeO_2 supporting catalytic systems are characterized by the fast transition between Ce^{4+} to Ce^{3+} that provides highly mobile O species, which can oxidize adsorbed S species

either on Ni or on CeO_2 . Similar processes have been identified with the aforementioned perovskite type materials especially with the presence of H_2O . Thus, the combination of a S tolerant supports and the presented strategy to modify the electronic and adsorption properties of Ni (e.g., with Au and Mo) toward a weakly bonded S can lead hopefully to S resistant electrodes.

CONCLUSIONS

In conclusion the present manuscript has given an overview of the activities of our group describing the roadmap for the deeper insight of the kinetics of the carbon deposition process during the steam reforming of CH_4 over Ni based SOFC cermet electrodes and the mitigation strategy followed in order to overcome the electrode degradation issues related to Carbon deposition and Sulfur poisoning. It appears that the key reaction steps that must be controlled in order to avoid carbon formation is to either retard the sequential dehydrogenation steps of CH_4 and the corresponding CH_x carbonaceous species or by blocking their further dehydrogenation by the oxidation of the latter species into CH_xO , which will end up into its dissociation forming CO and H_2 . The effect on the rate of these reaction steps was achieved by doping Ni with atomically dispersed Au or Au and Mo in order to affect its electronic properties and thus the adsorption strength and Kinetic constants of the aforementioned critical surface reaction steps. The most promising electrode appears to be Au₃-Mo₃-Ni/GDC, which also combines promising structural configurations, so as to optimize the extend of the electrochemical interface between Ni and GDC and the metal support interactions through the ability of the latter to activate oxygen or water and participate synergistically in the oxidation processes.

The enhanced properties of the ternary Au₃-Mo₃-Ni/GDC were also shown for its higher tolerance to sulfur poisoning. It seems that the ternary electrode has shifted the equilibrium of the desulfurization reaction toward H_2S formation, while the rate of H_2S dissociation on the ternary Au₃-Mo₃-Ni/GDC surface is being retarded.

AUTHOR CONTRIBUTIONS

SN is the leading scientist who coordinated and supervised the research activities that are being described in the manuscript. He was responsible for the organization of the manuscript. DN is a senior scientist who supervised and contributed significantly in the described research activities especially the Ni/GDC based materials. CN is doing his Ph.D. on both carbon and sulfur tolerant Au and Au/Mo modified Ni/GDC electrodes.

ACKNOWLEDGMENTS

The research leading to these results has received funding from (i) the INCO2-COPERNICUS2 programme of the European Commission under contract ICA2-CT-2000-10003, (ii) the

European Union's Sixth Framework Programme (FP6/2002-2006) under the project Real_SOFC IP project with Contract n° 502612 and (iii) from the Seventh Framework Programme

(FP7/2007-2013) for the Fuel Cells and Hydrogen Joint Technology Initiative under the projects **ROBANODE**, T-CELL with Grant Agreement n° [245355] and [298300], respectively.

REFERENCES

- An, W., Gatewood, D., Dunlap, B., and Turner, C. H. (2011). Catalytic activity of bimetallic nickel alloys for solid-oxide fuel cell anode reactions from density-functional theory. *J. Power Sources* 196, 4724–4728. doi: 10.1016/j.jpowsour.2011.01.007
- Atkinson, A., Barnett, S., Gorte, R. J., Irvine, J. T. S., McEvoy, A. J., Mogensen, M., et al. (2004). Advanced anodes for high-temperature fuel cells. *Nat. Mater.* 3, 17–27. doi: 10.1038/nmat1040
- Babaei, A., Jiang, S. P., and Li, J. (2009). Electrocatalytic promotion of palladium nanoparticles on hydrogen oxidation on Ni/GDC anodes of SOFCs via spillover. *J. Electrochem. Soc.* 156, B1022–B1029. doi: 10.1149/1.3156637
- Bebelis, S., Neophytides, S., Kotsionopoulos, N., Triantafyllopoulos, N., Colomer, M. T., and Jurado, J. (2006). Methane oxidation on composite ruthenium electrodes in YSZ cells. *Solid State Ionics* 177, 2087–2091. doi: 10.1016/j.ssi.2006.02.014
- Bebelis, S., Zeritis, A., Tiropani, C., and Neophytides, S. G. (2000). Intrinsic kinetics of the internal steam reforming of CH₄ over a Ni-YSZ-cermet catalyst-electrode. *Indus. Eng. Chem. Res.* 39, 4920–4927. doi: 10.1021/ie000350u
- Besenbacher, F., Chorkendorff, I., Clausen, B. S., Hammer, B., Molenbroek, A. M., Norskov, J. K., et al. (1998). Design of a surface alloy catalyst for steam reforming. *Science* 279, 1913–1915. doi: 10.1126/science.279.5358.1913
- Boaro, M., Modafferi, V., Pappacena, A., Llorca, J., Baglio, V., Frusteri, F., et al. (2010). Comparison between Ni-Rh/gadolinia doped ceria catalysts in reforming of propane for anode implementations in intermediate solid oxide fuel cells. *J. Power Sources* 195, 649–661. doi: 10.1016/j.jpowsour.2009.08.006
- Caillot, T., Gdlin, P., Dailly, J., Gauthier, G., Cayron, C., and Laurencin, J. (2007). Catalytic steam reforming of methane over La_{0.8}Sr_{0.2}CrO₃ based Ru catalysts. *Catal. Today* 128, 264–268. doi: 10.1016/j.cattod.2007.06.071
- Chen, H., Wang, F., Wang, W., Chen, D., Li, S.-D., and Shao, Z. (2016). H₂S poisoning effect and ways to improve sulfur tolerance of nickel cermet anodes operating on carbonaceous fuels. *Appl. Energy* 179, 765–777. doi: 10.1016/j.apenergy.2016.07.028
- Chen, T., Wang, W. G., Miao, H., Li, T., and Xu, C. (2011). Evaluation of carbon deposition behavior on the nickel/yttrium-stabilized zirconia anode-supported fuel cell fueled with simulated syngas. *J. Power Sources* 196, 2461–2468. doi: 10.1016/j.jpowsour.2010.11.095
- Cheng, Z., Wang, J.-H., Choi, Y., Yang, L., Lin, M. C., and Liu, M. (2011). From Ni-YSZ to sulfur-tolerant anode materials for SOFCs: electrochemical behavior, *in situ* characterization, modeling, and future perspectives. *Energy Environ. Sci.* 4, 4380–4409. doi: 10.1039/c1ee01758f
- Cheng, Z., Zha, S., and Liu, M. (2007). Influence of cell voltage and current on sulfur poisoning behavior of solid oxide fuel cells. *J. Power Sources* 172, 688–693. doi: 10.1016/j.jpowsour.2007.07.052
- Chin, Y.-H., King, D. L., Roh, H.-S., Wang, Y., and Heald, S. M. (2006). Structure and reactivity investigations on supported bimetallic AuNi catalysts used for hydrocarbon steam reforming. *J. Catal.* 244, 153–162. doi: 10.1016/j.jcat.2006.08.016
- Costa-Nunes, O., Gorte, R. J., and Vohs, J. M. (2005). Comparison of the performance of Cu-CeO₂-YSZ and Ni-YSZ composite SOFC anodes with H₂, CO, and syngas. *J. Power Sources* 141, 241–249. doi: 10.1016/j.jpowsour.2004.09.022
- da Paz Fiuza, R., Aurélio da Silva, M., and Boaventura, J. S. (2010). Development of Fe-Ni/YSZ-GDC electrocatalysts for application as SOFC anodes: XRD and TPR characterization and evaluation in the ethanol steam reforming reaction. *Int. J. Hydro. Energy* 35, 11216–11228. doi: 10.1016/j.ijhydene.2010.07.026
- Du, X., Zhang, D., Shi, L., Gao, R., and Zhang, J. (2012). Morphology dependence of catalytic properties of Ni/CeO₂ nanostructures for carbon dioxide reforming of methane. *J. Phys. Chem. C* 116, 10009–10016. doi: 10.1021/jp300543r
- European Fuel Cell Group and IEA Advanced Fuel Cell Programme (1994). *1st European Solid Oxide Fuel Cell Forum*. (Lucerne), 197–206.
- Faes, A., Hessler-Wyser, A., Presvytes, D., Vayenas, C. G., and Van herle, J. (2009). Nickel-zirconia anode degradation and triple phase boundary quantification from microstructural analysis. *Fuel Cells* 9, 841–851. doi: 10.1002/fuce.200800147
- Ferrandon, M., Kropf, A. J., and Krause, T. (2010). Bimetallic Ni-Rh catalysts with low amounts of Rh for the steam and autothermal reforming of n-butane for fuel cell applications. *Appl. Catal. A Gen.* 379, 121–128. doi: 10.1016/j.apcata.2010.03.013
- Finnerty, C. M., Coe, N. J., Cunningham, R. H., and Ormerod, R. M. (1998). Carbon formation on and deactivation of nickel-based/zirconia anodes in solid oxide fuel cells running on methane. *Catal. Today* 46, 137–145. doi: 10.1016/S0920-5861(98)00335-6
- Florea, M., Matei-Rutkowska, F., Postole, G., Urda, A., Neatu, F., Părvulescu, V. I., et al. (in press). Doped ceria prepared by precipitation route for steam reforming of methane. *Catal. Today*. doi: 10.1016/j.cattod.2016.12.006
- Fu, C. J., Chan, S. H., Ge, X. M., Liu, Q. L., and Pasciak, G. (2011). A promising Ni-Fe bimetallic anode for intermediate-temperature SOFC based on Gd-doped ceria electrolyte. *Int. J. Hydro. Energy* 36, 13727–13734. doi: 10.1016/j.ijhydene.2011.07.119
- Gavrielatos, I., Drakopoulos, V., and Neophytides, S. G. (2008). Carbon tolerant Ni-Au SOFC electrodes operating under internal steam reforming conditions. *J. Catal.* 259, 75–84. doi: 10.1016/j.jcat.2008.07.011
- Gong, M., Liu, X., Tremblay, J., and Johnson, C. (2007). Sulfur-tolerant anode materials for solid oxide fuel cell application. *J. Power Sources* 168, 289–298. doi: 10.1016/j.jpowsour.2007.03.026
- Goodenough, J. B., and Huang, Y.-H. (2007). Alternative anode materials for solid oxide fuel cells. *J. Power Sources* 173, 1–10. doi: 10.1016/j.jpowsour.2007.08.011
- Gorte, R. J., and Vohs, J. M. (2003). Novel SOFC anodes for the direct electrochemical oxidation of hydrocarbons. *J. Catal.* 216, 477–486. doi: 10.1016/S0021-9517(02)00121-5
- Gorte, R. J., Park, S., Vohs, J. M., and Wang, C. H. (2000). Anodes for direct oxidation of dry hydrocarbons in a solid-oxide fuel cell. *Adv. Mater.* 12, 1465–1469. doi: 10.1002/1521-4095(200010)12:19<1465::AID-ADMA1465>3.0.CO;2-9
- Hagen, A. (2013). Sulfur Poisoning of the water gas shift reaction on anode supported solid oxide fuel cells. *J. Electrochem. Soc.* 160, F111–F118. doi: 10.1149/2.060302jes
- Hagen, A., Rasmussen, J. F. B., and Thyden, K. (2011). Durability of solid oxide fuel cells using sulfur containing fuels. *J. Power Sources* 196, 7271–7276. doi: 10.1016/j.jpowsour.2011.02.053
- Hauch, A., Hagen, A., Hjelm, J., and Ramos, T. (2014). Sulfur poisoning of SOFC anodes: effect of overpotential on long-term degradation. *J. Electrochem. Soc.* 161, F734–F743. doi: 10.1149/2.080406jes
- Hibino, T., Hashimoto, A., Asano, K., Yano, M., Suzuki, M., and Sano, M. (2002a). An intermediate-temperature solid oxide fuel cell providing higher performance with hydrocarbons than with hydrogen. *Electrochem. Solid State Lett.* 5, A242–A244. doi: 10.1149/1.1508551
- Hibino, T., Hashimoto, A., Yano, M., Suzuki, M., and Sano, M. (2003). Ru-catalyzed anode materials for direct hydrocarbon SOFCs. *Electrochim. Acta* 48, 2531–2537. doi: 10.1016/S0013-4686(03)00296-2
- Hibino, T., Hashimoto, A., Yano, M., Suzuki, M., Yoshida, S., and Sano, M. (2002b). High performance anodes for SOFCs operating in methane-air mixture at reduced temperatures. *J. Electrochem. Soc.* 149, A133–A136. doi: 10.1149/1.1430226
- Hornés, A., Gamarra, D., Munuera, G., Conesa, J. C., and Martínez-Arias, A. (2007). Catalytic properties of monometallic copper and bimetallic copper-nickel systems combined with ceria and Ce-X (X = Gd, Tb) mixed oxides applicable as SOFC anodes for direct oxidation of methane. *J. Power Sources* 169, 9–16. doi: 10.1016/j.jpowsour.2007.01.074

- Huang, T.-J., Huang, M.-C., and Huang, M.-S. (2009). Novel methane steam-reforming catalyst of Ni-Bi₂O₃/GDC to reduce CO for hydrogen production. *Appl. Catal. A Gen.* 354, 127–131. doi: 10.1016/j.apcata.2008.11.020
- Huang, Y. H., Dass, R. I., Xing, Z. L., and Goodenough, J. B. (2006). Double perovskites as anode materials for solid-oxide fuel cells. *Science* 312, 254–257. doi: 10.1126/science.1125877
- Kan, H., and Lee, H. (2010a). Sn-doped Ni/YSZ anode catalysts with enhanced carbon deposition resistance for an intermediate temperature SOFC. *Appl. Catal. B Environ.* 97, 108–114. doi: 10.1016/j.catcom.2010.07.014
- Kan, H., and Lee, H. (2010b). Enhanced stability of Ni-Fe/GDC solid oxide fuel cell anodes for dry methane fuel. *Catal. Commun.* 12, 36–39. doi: 10.1016/j.apcatb.2010.03.029
- Kan, H., Hyun, S. H., Shul, Y.-G., and Lee, H. (2009). Improved solid oxide fuel cell anodes for the direct utilization of methane using Sn-doped Ni/YSZ catalysts. *Catal. Commun.* 11, 180–183. doi: 10.1016/j.catcom.2009.09.021
- Kim, H., Lu, C., Worrell, W. L., Vohs, J. M., and Gorte, R. J. (2002). Cu-Ni cermet anodes for direct oxidation of methane in solid-oxide fuel cells. *J. Electrochem. Soc.* 149, A247–A250. doi: 10.1149/1.1445170
- Koh, J.-H., Yoo, Y.-S., Park, J.-W., and Lim, H. C. (2002). Carbon deposition and cell performance of Ni-YSZ anode support SOFC with methane fuel. *Solid State Ionics* 149, 157–166. doi: 10.1016/S0167-2738(02)00243-6
- Konsolakis, M. (2016). The role of Copper–Ceria interactions in catalysis science: recent theoretical and experimental advances. *Appl. Catal. B Environ.* 198, 49–66. doi: 10.1016/j.apcatb.2016.05.037
- Kratzer, P., Hammer, B., and Nørskov, J. K. (1996). A theoretical study of CH₄ dissociation on pure and gold-alloyed Ni(111) surfaces. *J. Chem. Phys.* 105, 5595–5604. doi: 10.1063/1.472399
- Krishnan, V. V., McIntosh, S., Gorte, R. J., and Vohs, J. M. (2004). Measurement of electrode overpotentials for direct hydrocarbon conversion fuel cells. *Solid State Ionics* 166, 191–197. doi: 10.1016/j.ssi.2003.10.007
- Kromp, A., Dierickx, S., Leonide, A., Weber, A., and Ivers-Tiffée, E. (2012). Electrochemical analysis of sulphur-poisoning in anode-supported SOFCs under reformate operation. *ECS Trans.* 41, 161–169. doi: 10.1149/1.3702423
- Li, S., and Gong, J. (2014). Strategies for improving the performance and stability of Ni-based catalysts for reforming reactions. *Chem. Soc. Rev.* 43, 7245–7256. doi: 10.1039/C4CS00223G
- Li, T. S., and Wang, W. G. (2011a). The mechanism of H(2)S poisoning Ni/YSZ electrode studied by impedance spectroscopy. *Electrochem. Solid State Lett.* 14, B35–B37. doi: 10.1149/1.3526134
- Li, T. S., and Wang, W. G. (2011b). Sulfur-poisoned Ni-based solid oxide fuel cell anode characterization by varying water content. *J. Power Sources* 196, 2066–2069. doi: 10.1016/j.jpowsour.2010.10.015
- Li, T. S., Miao, H., Chen, T., Wang, W. G., and Xu, C. (2009). Effect of simulated coal-derived gas composition on H(2)S poisoning behavior evaluated using a disaggregation scheme. *J. Electrochem. Soc.* 156, B1383–B1388. doi: 10.1149/1.3232006
- Li, T. S., Wang, W. G., Chen, T., Miao, H., and Xu, C. (2010). Hydrogen sulfide poisoning in solid oxide fuel cells under accelerated testing conditions. *J. Power Sources* 195, 7025–7032. doi: 10.1016/j.jpowsour.2010.05.009
- Li, X., Zhao, H., Xu, N., Zhou, X., Zhang, C., and Chen, N. (2009). Electrical conduction behavior of La, Co co-doped SrTiO₃ perovskite as anode material for solid oxide fuel cells. *Int. J. Hydro. Energy* 34, 6407–6414. doi: 10.1016/j.ijhydene.2009.05.079
- Liu, J., Madsen, B. D., Ji, Z., and Barnett, S. A. (2002). A fuel-flexible ceramic-based anode for solid oxide fuel cells. *Electrochem. Solid State Lett.* 5, A122–A124. doi: 10.1149/1.1473258
- Maier, L., Schädel, B., Herrera Delgado, K., Tischer, S., and Deutschmann, O. (2011). Steam reforming of methane over nickel: development of a multi-step surface reaction mechanism. *Top. Catal.* 54, 845–858. doi: 10.1007/s11244-011-9702-1
- Matsui, T., Fujii, H., Ozaki, A., Takeuchi, T., Kikuchi, R., and Eguchi, K. (2007). Degradation behavior of Ni – ScSZ cermet anode under various humidified conditions for solid oxide fuel cells. *J. Electrochem. Soc.* 154, B1237–B1241. doi: 10.1149/1.2783771
- Matsui, T., Kishida, R., Kim, J.-Y., Muroyama, H., and Eguchi, K. (2010). Performance deterioration of Ni-YSZ anode induced by electrochemically generated steam in solid oxide fuel cells. *J. Electrochem. Soc.* 157, B776–B781. doi: 10.1149/1.3336830
- Modafferi, V., Panzera, G., Baglio, V., Frusteri, F., and Antonucci, P. L. (2008). Propane reforming on Ni-Ru/GDC catalyst: H₂ production for IT-SOFCs under SR and ATR conditions. *Appl. Catal. A Gen.* 334, 1–9. doi: 10.1016/j.apcata.2007.10.006
- Mogensen, D., Grunwaldt, J. D., Henriksen, P. V., Dam-Johansen, K., and Nielsen, J. U. (2011). Internal steam reforming in solid oxide fuel cells: status and opportunities of kinetic studies and their impact on modelling. *J. Power Sources* 196, 25–38. doi: 10.1016/j.jpowsour.2010.06.091
- Nabae, Y., Yamanaka, I., Hatano, M., and Otsuka, K. (2006). Catalytic behavior of Pd-Ni/composite anode for direct oxidation of methane in SOFCs. *J. Electrochem. Soc.* 153, A140–A145. doi: 10.1149/1.2136079
- Nabae, Y., Yamanaka, I., Hatano, M., and Otsuka, K. (2008). Mechanism of suppression of carbon deposition on the Pd-Ni/Ce(Sm)O-2-La(Sr)CrO₃ anode in dry CH₄ fuel. *J. Phys. Chem. C* 112, 10308–10315. doi: 10.1021/jp801496v
- Neofytidis, C., Athanasiou, M., Neophytides, S. G., and Niakolas, D. K. (2015). Sulfur tolerance of Au–Mo–Ni SOFC anodes under various CH₄ internal steam reforming conditions. *Top. Catal.* 58, 1276–1289. doi: 10.1007/s11244-015-0486-6
- Neofytidis, C., Dracopoulos, V., Neophytides, S. G., and Niakolas, D. K. (in press). Electrocatalytic performance and carbon tolerance of ternary Au-Mo-Ni/GDC SOFC anodes under CH₄-rich internal steam reforming conditions. *Catal. Today*. doi: 10.1016/j.cattod.2017.06.028
- Niakolas, D. K. (2014). Sulfur poisoning of Ni-based anodes for Solid Oxide Fuel Cells in H/C-based fuels. *Appl. Catal. A Gen.* 486, 123–142. doi: 10.1016/j.apcata.2014.08.015
- Niakolas, D. K., Athanasiou, M., Dracopoulos, V., Tsiaoussis, I., Bebelis, S., and Neophytides, S. G. (2013). Study of the synergistic interaction between nickel, gold and molybdenum in novel modified NiO/GDC cermets, possible anode materials for CH₄ fueled SOFCs. *Appl. Catal. A Gen.* 456, 223–232. doi: 10.1016/j.apcata.2013.02.024
- Niakolas, D. K., Neofytides, C., Neophytides, S. G., Tsiplakides, D., Papazisi, K.-M., and Balomenou, S. (2015). Carbon tolerant electrodes for SOFC and reversible SOFC (RSOFC) cells operating on carbon containing fuels. *ECS Trans.* 68, 3439–3447. doi: 10.1149/06801.3439ecst
- Niakolas, D. K., Ouweltjes, J. P., Rietveld, G., Dracopoulos, V., and Neophytides, S. G. (2010). Au-doped Ni/GDC as a new anode for SOFCs operating under rich CH₄ internal steam reforming. *Int. J. Hydro. Energy* 35, 7898–7904. doi: 10.1016/j.ijhydene.2010.05.038
- Nørskov, J. K., Abild-Pedersen, F., Studt, F., and Bligaard, T. (2011). Density functional theory in surface chemistry and catalysis. *Proc. Natl. Acad. Sci. U.S.A.* 108, 937–943. doi: 10.1073/pnas.1006652108
- Papaefthimiou, V., Shishkin, M., Niakolas, D. K., Athanasiou, M., Law, Y. T., Arrigo, R., et al. (2013). On the active surface state of nickel-ceria solid oxide fuel cell anodes during methane electrooxidation. *Adv. Energy Mater.* 3, 762–769. doi: 10.1002/aenm.201200727
- Park, H. C., and Virkar, A. V. (2009). Bimetallic (Ni-Fe) anode-supported solid oxide fuel cells with gadolinia-doped ceria electrolyte. *J. Power Sources* 186, 133–137. doi: 10.1016/j.jpowsour.2008.09.080
- Park, S. D., Vohs, J. M., and Gorte, R. J. (2000). Direct oxidation of hydrocarbons in a solid-oxide fuel cell. *Nature* 404, 265–267. doi: 10.1038/35005040
- Pujare, N. U., Semkow, K. W., and Sammells, A. F. (1987). A direct H₂S/air solid oxide fuel-cell. *J. Electrochem. Soc.* 134, 2639–2640. doi: 10.1149/1.2100262
- Ramirez-Cabrera, E., Atkinson, A., and Chadwick, D. (2004). Catalytic steam reforming of methane over Ce_{0.9}Gd_{0.1}O_{2-x}. *Appl. Catal. B Environ.* 47, 127–131. doi: 10.1016/j.apcatb.2003.08.008
- Rasmussen, J. F. B., and Hagen, A. (2009). The effect of H₂S on the performance of Ni-YSZ anodes in solid oxide fuel cells. *J. Power Sources* 191, 534–541. doi: 10.1016/j.jpowsour.2009.02.001
- Rasmussen, J. F. B., and Hagen, A. (2010). The effect of H(2)S on the performance of SOFCs using methane containing fuel. *Fuel Cells* 10, 1135–1142. doi: 10.1002/uce.201000012
- Rostrup-Nielsen, J. R., and Alstrup, I. (1999). Innovation and science in the process industry: steam reforming and hydrogenolysis. *Catal. Today* 53, 311–316. doi: 10.1016/S0920-5861(99)00125-X
- Ruiz-Morales, J. C., Canales-Vázquez, J., Ballesteros-Pérez, B., Pérez, Pea-Martínez, J., Marrero-López, D., Irvine, J. T. S., et al. (2007). LSCM-(YSZ-CGO) composites as improved symmetrical electrodes for solid oxide fuel cells. *J. Eur. Ceram. Soc.* 27, 4223–4227. doi: 10.1016/j.jeurceramsoc.2007.02.117

- Sasaki, K., Haga, K., Yoshizumi, T., Minematsu, D., Yuki, E., Liu, R., et al. (2011). Chemical durability of Solid Oxide Fuel Cells: influence of impurities on long-term performance. *J. Power Sources* 196, 9130–9140. doi: 10.1016/j.jpowsour.2010.09.122
- Sasaki, K., Susuki, K., Iyoshi, A., Uchimura, M., Imamura, N., Kusaba, H., et al. (2006). H₂S poisoning of solid oxide fuel cells. *J. Electrochem. Soc.* 153, A2023–A2029. doi: 10.1149/1.2336075
- Sauvet, A.-L., and Fouletier, J. (2001). Electrochemical properties of a new type of anode material La_{1-x}Sr_xCr_{1-y}Ru_yO_{3-δ} for SOFC under hydrogen and methane at intermediate temperatures. *Electrochim. Acta* 47, 987–995. doi: 10.1016/S0013-4686(01)00811-8
- Sfeir, J., Buffat, P. A., Möchli, P., Xanthopoulos, N., Vasquez, R., Mathieu, H. J., et al. (2001). Lanthanum chromite based catalysts for oxidation of methane directly on SOFC anodes. *J. Catal.* 202:229. doi: 10.1006/jcat.2001.3286
- Sin, A., Kopnin, E., Dubitsky, Y., Zaopo, A., Aricò, A. S., La Rosa, D., et al. (2007). Performance and life-time behaviour of NiCu-CGO anodes for the direct electro-oxidation of methane in IT-SOFCs. *J. Power Sources* 164, 300–305. doi: 10.1016/j.jpowsour.2006.10.078
- Singh, A., and Hill, J. M. (2012). Carbon tolerance, electrochemical performance and stability of solid oxide fuel cells with Ni/yttria stabilized zirconia anodes impregnated with Sn and operated with methane. *J. Power Sources* 214, 185–194. doi: 10.1016/j.jpowsour.2012.04.062
- Slater, P. R., and Irvine, J. T. S. (1999). Synthesis and electrical characterisation of the tetragonal tungsten bronze type phases, (Ba/Sr/Ca/La)₀ 6MxNb_{1-x}O₃-[delta] (M=Mg, Ni, Mn, Cr, Fe, In, Sn): evaluation as potential anode materials for solid oxide fuel cells. *Solid State Ionics* 124, 61–72. doi: 10.1016/S0167-2738(99)00127-7
- Smith, B. H., and Gross, M. D. (2011). A highly conductive oxide anode for solid oxide fuel cells. *Electrochem. Solid State Lett.* 14, B1–B5. doi: 10.1149/1.3505101
- Souentie, S., Athanasiou, M., Niakolas, D. K., Katsaounis, A., Neophytides, S. G., and Vayenas, C. G. (2013). Mathematical modeling of Ni/GDC and Au-Ni/GDC SOFC anodes performance under internal methane steam reforming conditions. *J. Catal.* 306, 116–128. doi: 10.1016/j.jcat.2013.06.015
- Subotić, V., Schluckner, C., Schroettner, H., and Hochenauer, C. (2016b). Analysis of possibilities for carbon removal from porous anode of solid oxide fuel cells after different failure modes. *J. Power Sources* 302, 378–386. doi: 10.1016/j.jpowsour.2015.10.071
- Subotić, V., Schluckner, C., Strasser, J., Lawlor, V., Mathe, J., Rechberger, J., et al. (2016a). *In-situ* electrochemical characterization methods for industrial-sized planar solid oxide fuel cells Part I: methodology, qualification and detection of carbon deposition. *Electrochim. Acta* 207, 224–236. doi: 10.1016/j.electacta.2016.05.025
- Sun, C., and Stimming, U. (2007). Recent anode advances in solid oxide fuel cells. *J. Power Sources* 171, 247–260. doi: 10.1016/j.jpowsour.2007.06.086
- Tao, S. W., and Irvine, J. T. S. (2004). Synthesis and characterization of (La_{0.75}Sr_{0.25})Cr_{0.5}Mn_{0.5}O₃-delta, a redox-stable, efficient perovskite anode for SOFCs. *J. Electrochem. Soc.* 151, A252–A259. doi: 10.1149/1.1639161
- Tremblay, J. P., Marquez, A. I., Ohn, T. R., and Bayless, D. J. (2006). Effects of coal syngas and H₂S on the performance of solid oxide fuel cells: single-cell tests. *J. Power Sources* 158, 263–273. doi: 10.1016/j.jpowsour.2005.09.055
- Triantafyllopoulos, N. C., and Neophytides, S. G. (2003). The nature and binding strength of carbon adspecies formed during the equilibrium dissociative adsorption of CH₄ on Ni-YSZ cermet catalysts. *J. Catal.* 217, 324–333. doi: 10.1016/S0021-9517(03)00062-9
- Triantafyllopoulos, N. C., and Neophytides, S. G. (2006). Dissociative adsorption of CH₄ on NiAu/YSZ: the nature of adsorbed carbonaceous species and the inhibition of graphitic C formation. *J. Catal.* 239, 187–199. doi: 10.1016/j.jcat.2006.01.021
- Tsipsi, E. V., and Kharton, V. V. (2008). Electrode materials and reaction mechanisms in solid oxide fuel cells: a brief review. *J. Solid State Electrochem.* 12, 1367–1391. doi: 10.1007/s10008-008-0611-6
- Vashook, V., Vasylechko, L., Zosel, J., and Guth, U. (2003). Synthesis, crystal structure, and transport properties of La_{1-x}CaxCr_{0.5}Ti_{0.5}O₃-[delta]. *Solid State Ionics* 159, 279–292. doi: 10.1016/S0167-2738(03)00103-6
- Vayenas, C. G., Bebelis, S., Pliangos, C., Brosda, S., and Tsiplakides, D. (2001). *Electrochemical Activation of Catalysis: Promotion, Electrochemical Promotion and Metal-Support Interactions*. Kluwer New York, NY: Academic/Plenum Publishers.
- Vorontsov, V., An, W., Luo, J. L., Sanger, A. R., and Chuang, K. T. (2008). Performance and stability of composite nickel and molybdenum sulfide-based anodes for SOFC utilizing H₂S. *J. Power Sources* 179, 9–16. doi: 10.1016/j.jpowsour.2007.12.097
- Wang, F., Wang, W., Qu, J., Zhong, Y., Tade, M. O., and Shao, Z. (2014). Enhanced sulfur tolerance of nickel-based anodes for oxygen-ion conducting solid oxide fuel cells by incorporating a secondary water storing phase. *Environ. Sci. Technol.* 48, 12427–12434. doi: 10.1021/es503603w
- Wang, W., Su, C., Wu, Y., Ran, R., and Shao, Z. (2013). Progress in solid oxide fuel cells with nickel-based anodes operating on methane and related fuels. *Chem. Rev.* 113, 8104–8151. doi: 10.1021/cr300491e
- Weaver, D., and Winnick, J. (1989). Sulfation of the molten carbonate fuel-cell anode. *J. Electrochem. Soc.* 136, 1679–1686. doi: 10.1149/1.2096992
- Weber, A., Dierickx, S., Kromp, A., and Ivers-Tiffée, E. (2013). Sulfur poisoning of anode-supported SOFCs under reformat operation. *Fuel Cells* 13, 487–493. doi: 10.1002/fuce.201200180
- Wu, H., La Parola, V., Pantaleo, G., Puleo, F., Venezia, A., and Liotta, L. (2013). Ni-based catalysts for low temperature methane steam reforming: recent results on Ni-Au and comparison with other Bi-metallic systems. *Catalysts* 3:563. doi: 10.3390/catal3020563
- Xiao, G., Liu, Q., Dong, X., Huang, K., and Chen, F. (2010). Sr₂Fe₄/3Mo₂/3O₆ as anodes for solid oxide fuel cells. *J. Power Sources* 195, 8071–8074. doi: 10.1016/j.jpowsour.2010.07.036
- Xu, C., Zondlo, J. W., Gong, M., Elizalde-Blancas, F., Liu, X., and Celik, I. B. (2010). Tolerance tests of H₂S-laden biogas fuel on solid oxide fuel cells. *J. Power Sources* 195, 4583–4592. doi: 10.1016/j.jpowsour.2010.02.078
- Yang, L., Cheng, Z., Liu, M., and Wilson, L. (2010). New insights into sulfur poisoning behavior of Ni-YSZ anode from long-term operation of anode-supported SOFCs. *Energy Environ. Sci.* 3, 1804–1809. doi: 10.1039/c0ee00386g
- Ye, X.-F., Huang, B., Wang, S. R., Wang, Z. R., Xiong, L., and Wen, T. L. (2007). Preparation and performance of a Cu-CeO₂-ScSZ composite anode for SOFCs running on ethanol fuel. *J. Power Sources* 164, 203–209. doi: 10.1016/j.jpowsour.2006.10.056
- Yentekakis, I. V. (2006). Open- and closed-circuit study of an intermediate temperature SOFC directly fueled with simulated biogas mixtures. *J. Power Sources* 160, 422–425. doi: 10.1016/j.jpowsour.2005.12.069
- Yentekakis, I. V., and Vayenas, C. G. (1989). Chemical cogeneration in solid electrolyte cells - the oxidation of H₂S TO SO₂. *J. Electrochem. Soc.* 136, 996–1002. doi: 10.1149/1.2096899
- Yentekakis, I. V., Papadam, T., and Goula, G. (2008). Electricity production from wastewater treatment via a novel biogas-SOFC aided process. *Solid State Ionics* 179, 1521–1525. doi: 10.1016/j.ssi.2007.12.049
- Zha, S., Cheng, Z., and Liu, M. (2007). Sulfur poisoning and regeneration of Ni-based anodes in solid oxide fuel cells. *J. Electrochem. Soc.* 154, B201–B206. doi: 10.1149/1.2404779
- Zhang, P., Huang, Y.-H., Cheng, J.-G., Mao, Z.-Q., and Goodenough, J. B. (2011). Sr₂CoMoO₆ anode for solid oxide fuel cell running on H₂ and CH₄ fuels. *J. Power Sources* 196, 1738–1743. doi: 10.1016/j.jpowsour.2010.10.007

Conflict of Interest Statement: The authors declare that the research was conducted in the absence of any commercial or financial relationships that could be construed as a potential conflict of interest.

The reviewer MK and handling Editor declared their shared affiliation.

Copyright © 2017 Niakolas, Neofytidis and Neophytides. This is an open-access article distributed under the terms of the Creative Commons Attribution License (CC BY). The use, distribution or reproduction in other forums is permitted, provided the original author(s) or licensor are credited and that the original publication in this journal is cited, in accordance with accepted academic practice. No use, distribution or reproduction is permitted which does not comply with these terms.